MASTER

A Magnetic Spectrograph for the Holifield Heavy Ion Research Facility

J.L.C. Ford, Jr.
H. A. Enge
J. R. Erskine
D. L. Hendrie
M. J. LeVine

OAK RIDGE NATIONAL LABORATORY

BLANK PAGE

Contract No. W-7405-eng-26

PHYSICS DIVISION

A MAGNETIC SPECTROGRAPH FOR THE HOLIFIELD HEAVY ION RESEARCH FACILITY

J. L. C. Ford, Jr.
H. A. Enge
J. R. Erskine
D. L. Hendrie
M. J. LeVine

Date Published: January 1977

CONTENTS

ACKNOWLEDGEMENTS

A MAGNETIC SPECTROGRAPH FOR THE HOLIFIELD HEAVY ION RESEARCH FACILITY

J. L. C. Ford, Jr.[*]
Oak Ridge National Laboratory

H. A. Enge[**]
Physics Department and Laboratory for Nuclear Science
Massachusetts Institute of Technology

J. R. Erskine[†]
Argonne National Laboratory

D. L. Hendrie[†]
Lawrence Berkeley Laboratory

and

M. J. LeVine[†]
Brookhaven National Laboratory

ABSTRACT

This report presents the need for a new generation magnetic spectrograph for the Holifield Heavy Ion Research Facility. The advantages of a magnetic spectrograph for heavy ion research are discussed, as well as some of the types of experiments for which such an instrument is suited. The limitations which the quality of the incident beam, target and spectrograph itself impose on high resolution heavy ion measurements are discussed. Desired features of an ideal new spectrograph are:

intrinsic resolving power	$E/\Delta E \geq 3000.$
maximum solid angle	≥ 20 msr.
dispersion	~ 4-8m
maximum energy interval	$\sim 30\%.$
mass-energy product	≥ 200

Various existing and proposed spectrographs are compared with the specifications for a new heavy ion magnet design.

BLANK PAGE

I. INTRODUCTION

The 25 MV tandem accelerator, presently under construction at the Oak Ridge National Laboratory, together with the existing cyclotron as an energy booster will provide scientists with a powerful new facility for heavy ion research. The new tandem will accelerate ion beams with the high resolution, excellent beam qualities, and ease of energy variability associated with electrostatic machines. Since one of the unique features of the new heavy ion tandem as compared to other heavy ion accelerators will be its high energy resolution, a new generation magnetic spectrograph will be needed in order to exploit this capability of the accelerator. This report then briefly discusses the research potential, energy resolution limitations, and desirable characteristics of a heavy ion magnetic spectrograph.

II. ADVANTAGES OF A SPECTROGRAPH FOR HEAVY ION RESEARCH

Heavy ion reactions are typically characterized by the fact that a large number of different products are emitted. This fact not only usually results in a small cross section for any given exit channel of interest, but also means that it is necessary to distinguish between the large number of different Z and A values produced. Proper identification demands that several parameters, such as energy and energy loss, be measured with good resolution. However, the large energy shift with angle in heavy ion reactions necessitates detection apparatus capable of kinematic compensation in order to simultaneously have good energy resolution and a large solid angle.

For many types of heavy ion research a magnetic spectrograph provides the best solution for the above problems since a spectrograph may have the following important properties:

A. High Energy Resolution. A spectrograph can provide an energy resolution $\Delta E/E$ between 10^{-3} and 10^{-4} over a relatively large energy span and with good solid angle. The capability of a magnetic spectrograph to perform high resolution experiments with heavy ions from either a cyclotron or tandem accelerator is demonstrated in Figs. 1 and 2 which, respectively,[1,2] show spectra for inelastic scattering of ^{12}C ions from the Berkeley 88 inch cyclotron as measured with the QSD spectrograph[3,4] ($\Delta E = 60$ keV or $E/\Delta E = 1300$), and for the (^{12}C,^{14}C) reaction measured at the Brookhaven MP tandem with a Q3D spectrograph[5,6] ($\Delta E = 48$ keV or $E/\Delta E \approx 1350$). For comparison, the energy resolution for heavy ions for carbon or above is limited to about 0.1% greater with solid state counters,[7] and up to present to about 0.7% with ionization chambers (see for example Ref. 8). In addition, solid state counters are very subject to radiation damage under heavy ion bombardment. Time-of-flight systems not only have a limited energy resolution, but typically small solid angles as well.

B. Particle Identification. The large variety of different reaction products which may be formed in heavy ion reactions make it essential to be able to clearly identify and distinguish between the many possible particles which may be emitted. The use of active focal-plane detectors permitting the measurement of parameters such as the energy, energy loss, position, angle of incidence, and time-of-flight
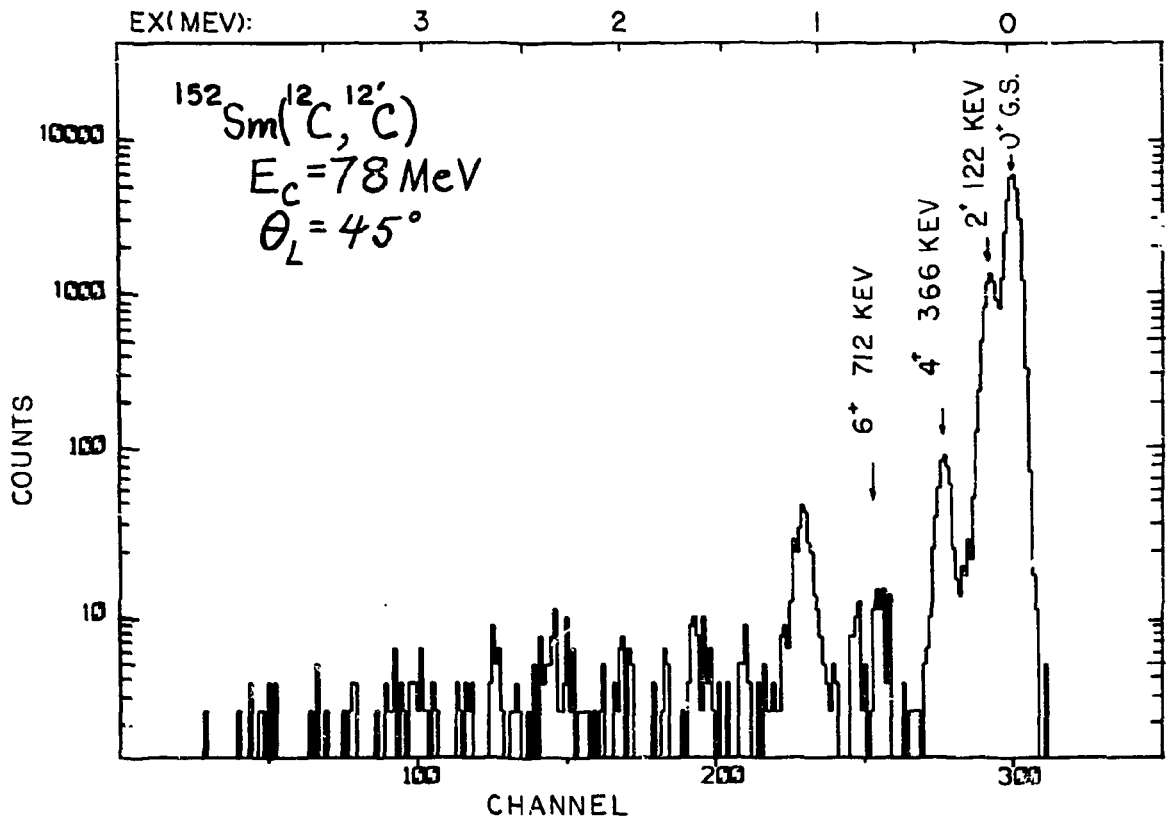
Fig. 1. The ^{12}C spectrum from inelastic scattering of ^{12}C from ^{152}Sm at a laboratory energy of 78 MeV (Ref. 1).
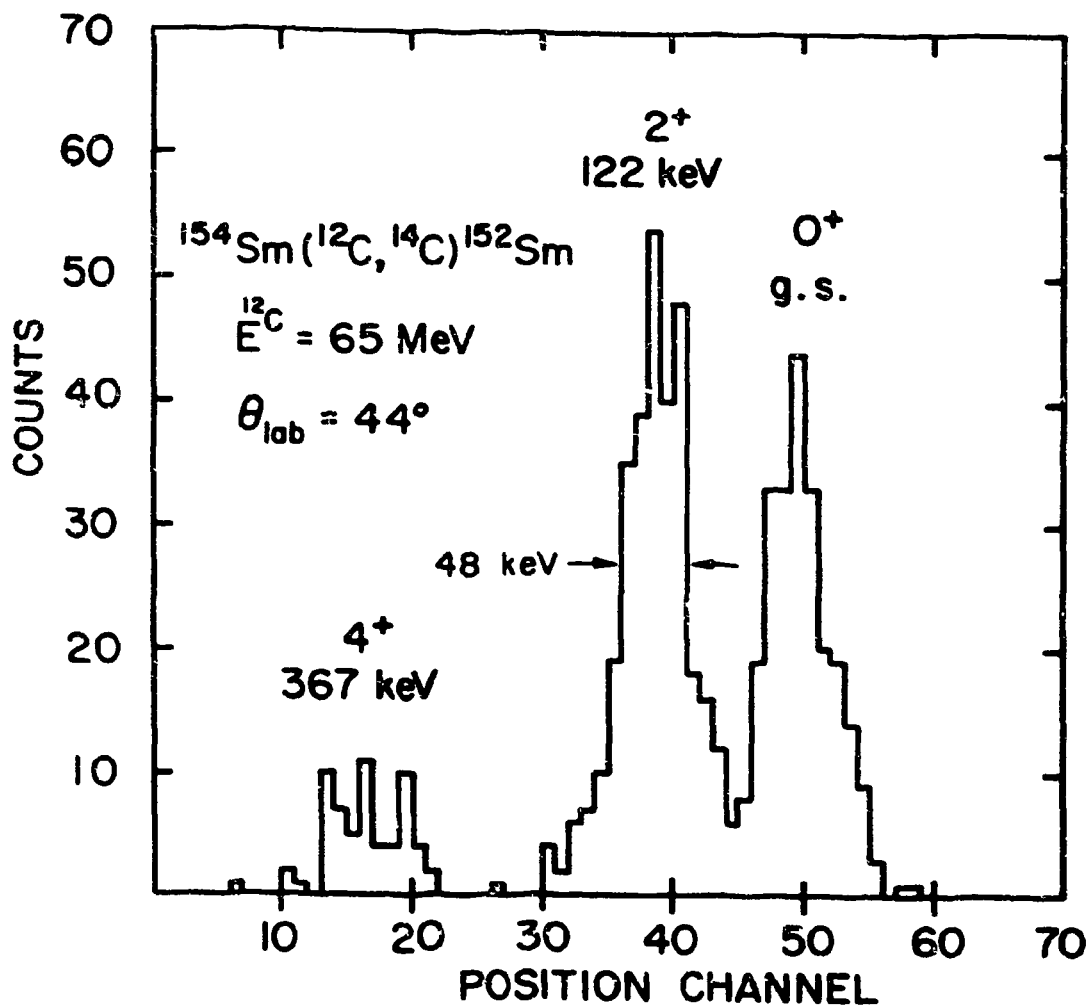
Fig. 2. Spectrum from the reaction $^{154}Sm(^{12}C,^{14}C)^{152}Sm$ taken at $\theta_{lab} = 44°$ and for a beam energy of 65 MeV (Ref. 2).

through the spectrograph have revolutionized work with magnetic spectrographs in recent years. Such detectors have made the magnetic spectrograph an unmatched instrument for particle identification. For example, Fig. 3 shows a time-of-flight versus energy-loss plot obtained at the Berkeley cyclotron by bombarding ^{24}Mg with 86 MeV ^{11}B ions in which the position and energy loss were measured with a 60-cm long, position-sensitive proportional counter, and time-of-flight with a plastic scintillator following the gas counter.[9,10] Recent work with position-sensitive devices based on ionization chambers indicate that ΔE and E measurements can be made with a resolution of about 3-5%, depending on the ion and its energy, and 1%, respectively, permitting the determination of the reaction angle, energy, atomic number, charge state, and mass for ions as heavy as at least A = 40.[8,11] Figure 4 illustrates the excellent separation of the different masses and charge states of carbon isotopes possible with the Argonne National Laboratory device of this type when observing reaction products due to 56 MeV ^{16}O ions incident on a target of ^{48}Ca [Ref. 8]. It can be expected that there will continue to be rapid development and refinement of large gaseous focal plane detectors. These counters have so extended the research potential of magnetic spectrographs that the spectrograph and its associated detector must be considered together as a system. Indeed, the properties of the detector will strongly influence the desired characteristics of a new spectrograph as discussed in Section V.
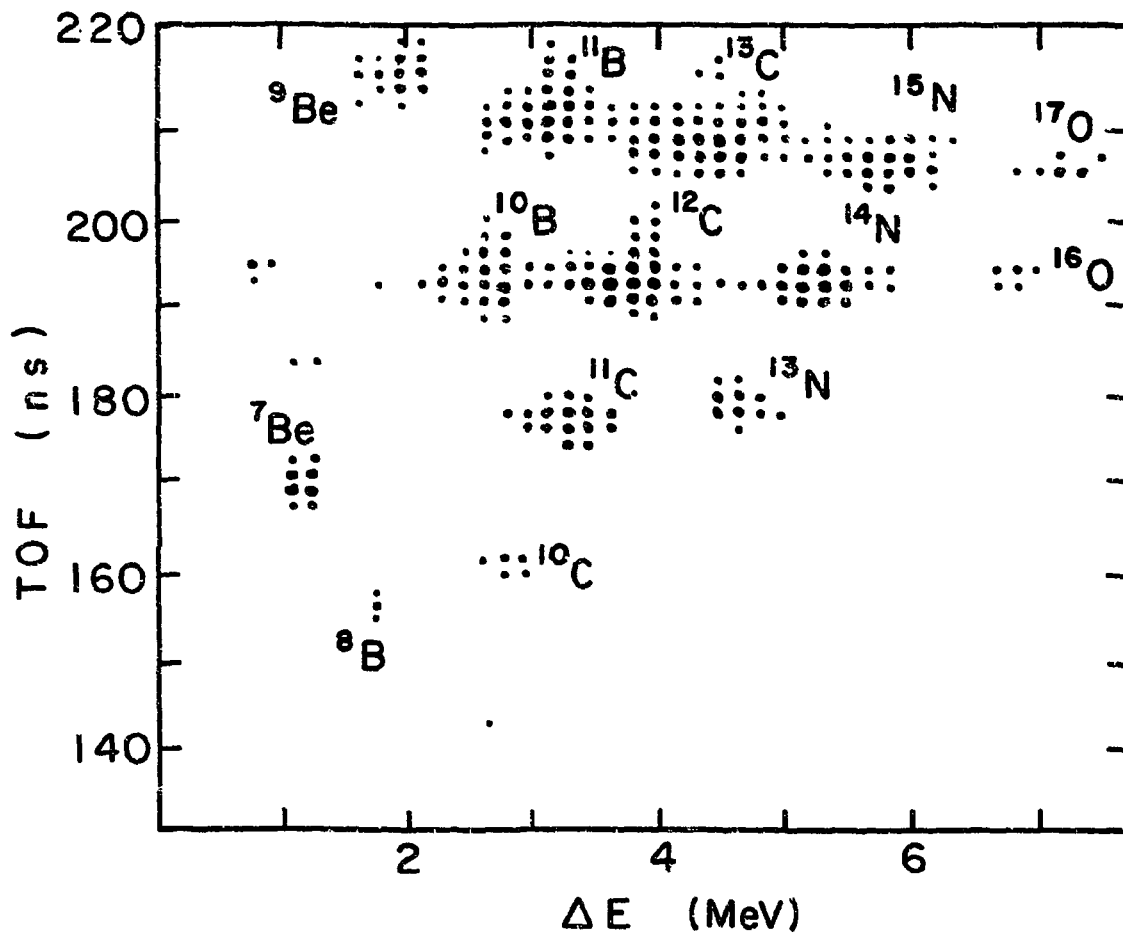
XBL744-2896

Fig. 3. A plot of time-of-flight versus ΔE obtained by bombarding
^{24}Mg with 86 MeV ^{11}B ions (Ref. 9).
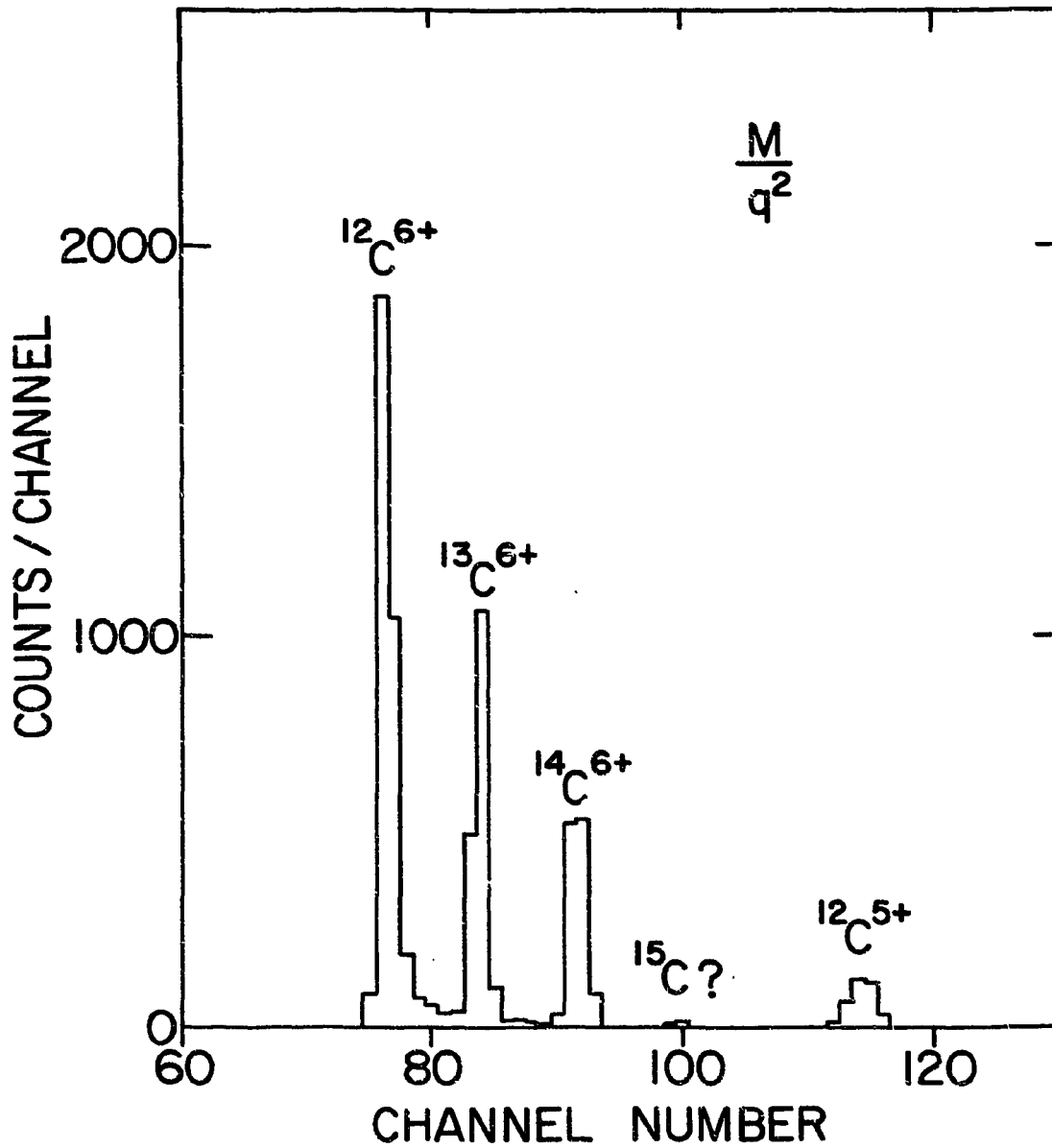
Fig. 4. The m/q^2 spectrum measured with a 56-MeV ^{16}O beam bombarding a target of ^{48}Ca. A window has been set in $\Delta E \cdot E$ space to select only carbon events. The ^{12}C ions were not fully stopped in the detector, which caused the tail on the right side of the $^{12}C^{6+}$ peak (Ref. 8).

C. <u>Large Solid Angle.</u> Spectrographs with solid angles as large as 15 msr are in use today. Such solid angles are essential in order to measure heavy ion reactions having small cross sections. However, a large solid angle is not useful unless the variation with angle of the energy of the emitted particle is corrected since otherwise the energy resolution is smeared. Magnetic spectrographs can be designed to compensate for this kinematic energy shift even for reactions for which the center-of-mass motion is large. On the other hand the angular distribution of many heavy-ion reactions show fine structure such as closely spaced oscillations. This makes a large horizontal entrance angle not fully useful unless some means of electronically measuring the angle of the detected particle and sorting of the data by angle can be performed during analysis. However, modern focal plane counters (e.g. Refs. 8 and 11) can measure the trajectories of the detected particles so that the angle at which a particle enters the spectrograph entrance window can be measured with an angular resolution as fine as 7 milliradians.[12] Such measurements not only make it possible to study details in heavy ion angular distributions but also to correct for aberrations of the magnet as well as effects in time-of-flight spectra due to the different particle paths within the spectrograph.

D. <u>Zero Degree Measurements and Background Suppression.</u> A magnetic device serves to filter out many of the reaction products which are not of interest so that weak processes can be observed. This feature is particularly important for heavy ion studies since the reactions predominantly occur at very forward angles where the effects due to

small angle slit scattering, and the intense elastic scattering peak for heavy ion interactions must be removed. In particular, a magnet makes possible measurements at 0 degrees an angle of great importance in many angular correlation studies. In many coincidence experiments a single high resolution leg is sufficient and in these cases a high resolution spectrograph may make it possible to replace a low efficiency Ge(Li) gamma-ray detector with a higher efficiency NaI counter.

Although the above four characteristics of magnetic spectrographs are their most important features for heavy ion work, they do not exhaust the advantages that magnetic systems have for research. When the spectrograph would be used with the ORIC cyclotron rather than the 25 MV tandem beam, it is advantageous to do dispersion matching[13] between the spectrometer and beam analysis system in order to improve the energy resolution beyond that directly available with the cyclotron beam. Yet another useful property is the ability to separate the different charge states with which a given ion emerges from the target material. This separation of charge states has been used in atomic physics investigations on the dependence of the energy loss of ions on their initial charge state. This property can also be a disadvanage for heavy ions, however, due to the number of charge states which one may have to measure in order to determine a cross section.

III. RESEARCH POTENTIAL OF A SPECTROGRAPH

The properties of magnetic spectrograph systems discussed in Section II make it clear that such a system is a powerful and indeed

essential tool for heavy ion research. While it is difficult to foresee the direction heavy ion work might have taken by the time a new generation spectrograph is operational at the Holifield Heavy Ion Research Facility, a brief discussion will be given of some of the fields in which magnetic spectrographs have already greatly contributed in order to illustrate their potential as a research tool.

A. Elastic Scattering. A magnetic spectrograph system has the unique capability of clearly selecting any desired reaction channel. In many situations critical tests of theory cannot be made without complete separation of the reaction channel of interest. For example, the basic measurement of the elastic scattering cross section at high energy with very heavy-ions is not easy to do without good energy resolution, since low-lying excited states of either the projectile or target must not be included in the cross section.

B. Coulomb Excitation. This field, which has provided a powerful technique for investigating the shapes of nuclei as well as determining static and transition moments with which to test collective models of the nucleus, will profit as still heavier projectiles become available. The ^{232}Th spectrum for inelastic α-particle scattering shown in Fig. 5 [Ref. 14] was measured with a position sensitive proportional detector at the focal plane of the split pole spectrograph[15] at the ORNL tandem accelerator. This figure illustrates the high resolution, background free spectra which can be obtained with spectrographs and which are essential in studying collective nuclei.
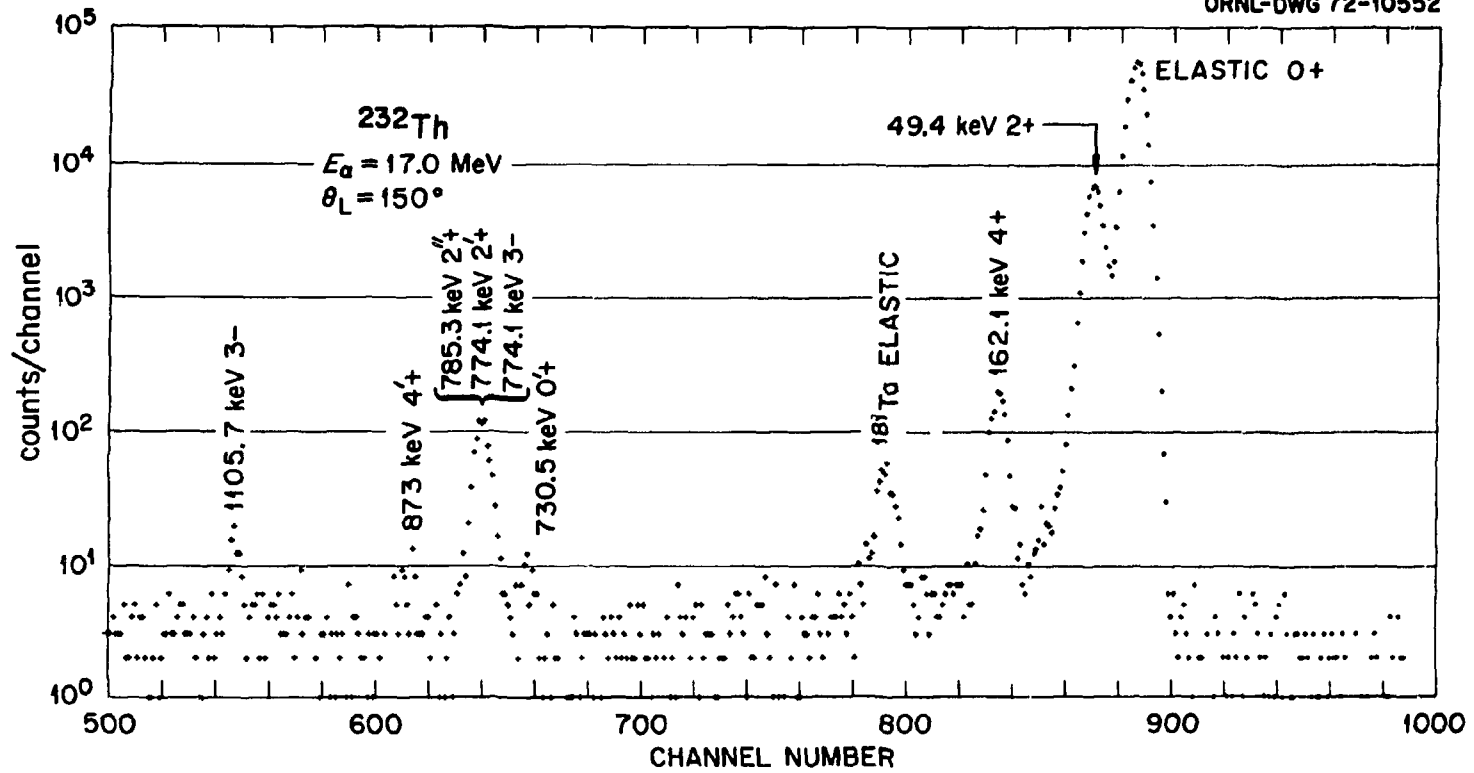
Fig. 5. Elastically and inelastically scattered 17-MeV ^{4}He ions from ^{232}Th at a laboratory angle of 150° using a carbon foil as the target backing. Peak-to-background ratio is ~ 20,000 to 1. The ^{181}Ta contamination is from the $Ta^{16}O^{35}Cl^+$ molecular ion which was collected at the ^{232}Th position in the isotope separator used to make the target (Ref. 14).

C. **Nuclear Inelastic Scattering.** Heavy ion inelastic scattering above the Coulomb barrier appears to also be a sensitive method for measuring nuclear deformations and matrix elements such as those due to reorientation effects. It is also an important technique for gaining insight into the reaction mechanism. Figure 6 shows angular distributions for inelastic scattering of 70.4 MeV ^{12}C ions from ^{144}Nd [Ref. 16] measured with the Elbek spectrograph[17,18] and a position sensitive proportional counter at the ORIC cyclotron. The dashed and solid lines in the figure are the result of DWBA and coupled-channels calculations and indicate the importance of multistep processes in such heavy ion reactions. Nuclear inelastic scattering with heavy ions may make it possible to excite states with high angular momentum, and to investigate the applicability of various microscopic models in order to reproduce elastic and inelastic data. However, such studies will require the good resolution and large solid angle that magnetic spectrographs can supply.

D. **Selectivity of Highly Excited States.** Since heavy ion reactions involve large angular momentum, they have proved to be a significant means with which to selectively populate high spin states in residual nuclei populated in compound nucleus reactions. This characteristic is illustrated in Fig. 7 showing the levels observed in the ^{12}C(^{16}O,α) reaction at 46 MeV and an angle of 7°(lab) using the split-pole spectrograph at the ORNL tandem.[19] This figure also indicates the ability of a spectrograph to measure good resolution spectra which extend over a wide range of energies of the detected particle. When

ORNL-DWG 75-13956R
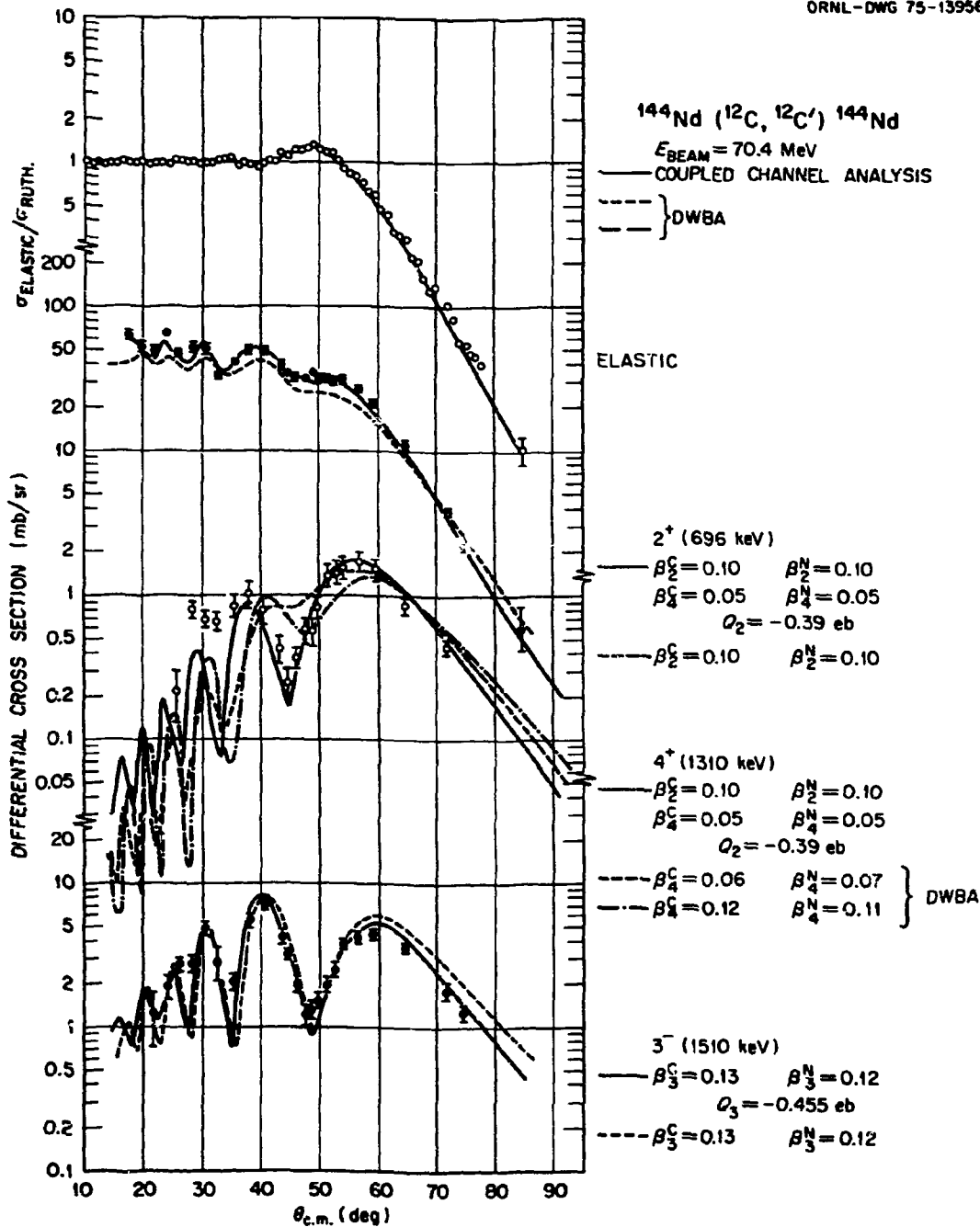
Fig. 6. Coupled channel calculations (solid curves) of the differential cross sections for 70.4 MeV ^{12}C ions scattered from ^{144}Nd in comparison with single step DWBA calculations (dashed curves). The deformation lengths are equal in all calculations (Rev. 16).
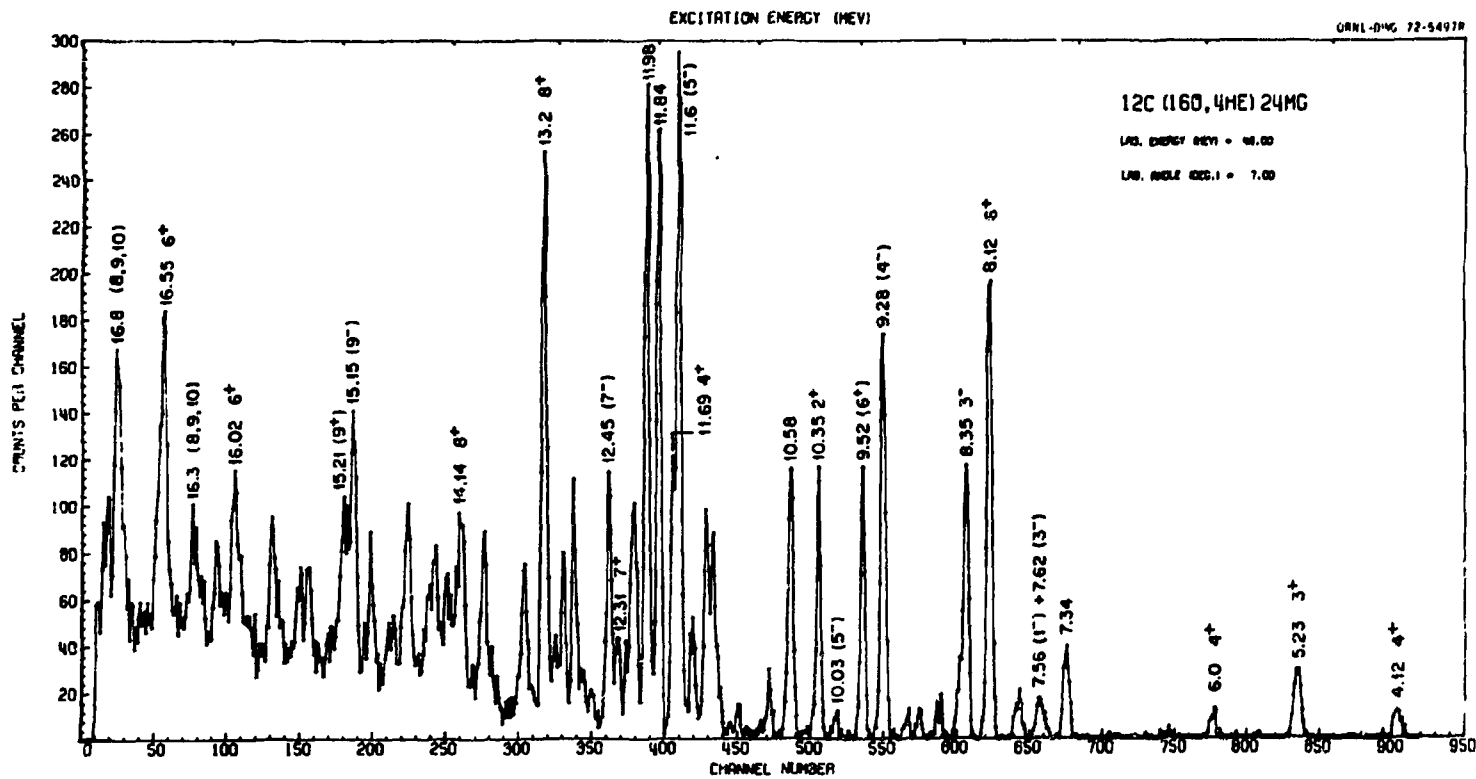
Fig. 7. An α-particle spectrum from the $^{12}C(^{16}O,\alpha)$ reaction at a laboratory angle and energy of 7° and 46 MeV, respectively (Ref. 19).

heavier and more energetic heavy ions are available from the new tandem, these advantages of a spectrograph will become still more important in order to search for highly excited states which are populated because of their high spin or unusual character.

E. Many Particle Transfer Reactions. A particular advantage of heavy ions in contrast to light ions is the fact that many nucleons can be transferred in a reaction. Figure 8 displays the two proton transfer reaction ($^{16}O,^{14}C$) on ^{48}Ca as measured with an ionization type focal plane detector and the split pole spectrograph at the Argonne tandem.[8] Note the high resolution (E/ΔE $\sim$ 780) limited by target effects, the low background and large energy bite covered in the spectrum. A case where as many as 8 nucleons are transferred due to a direct reaction mechanism is in the $^{12}C(^{12}C,\alpha)^{20}Ne$ reaction. Figure 9 shows spectra at various energies for this reaction as also measured at ANL.[20] As it becomes possible to use heavy ions with higher bombarding energies, restrictions on many particle transfer reactions due to the Coulomb barrier disappear. New effects such as due to possible superfluid properties of nuclei will be accessible for investigation. However, good energy resolution and low background will be essential.

F. Multi-step Processes in Reactions. Heavy ions increase the likelihood of multi-step processes in not only inelastic scattering but in all types of reactions as well. Figure 10 shows experimental and calculated (CCBA) angular distributions for transitions leading to the first three members of the ground-state rotational band of
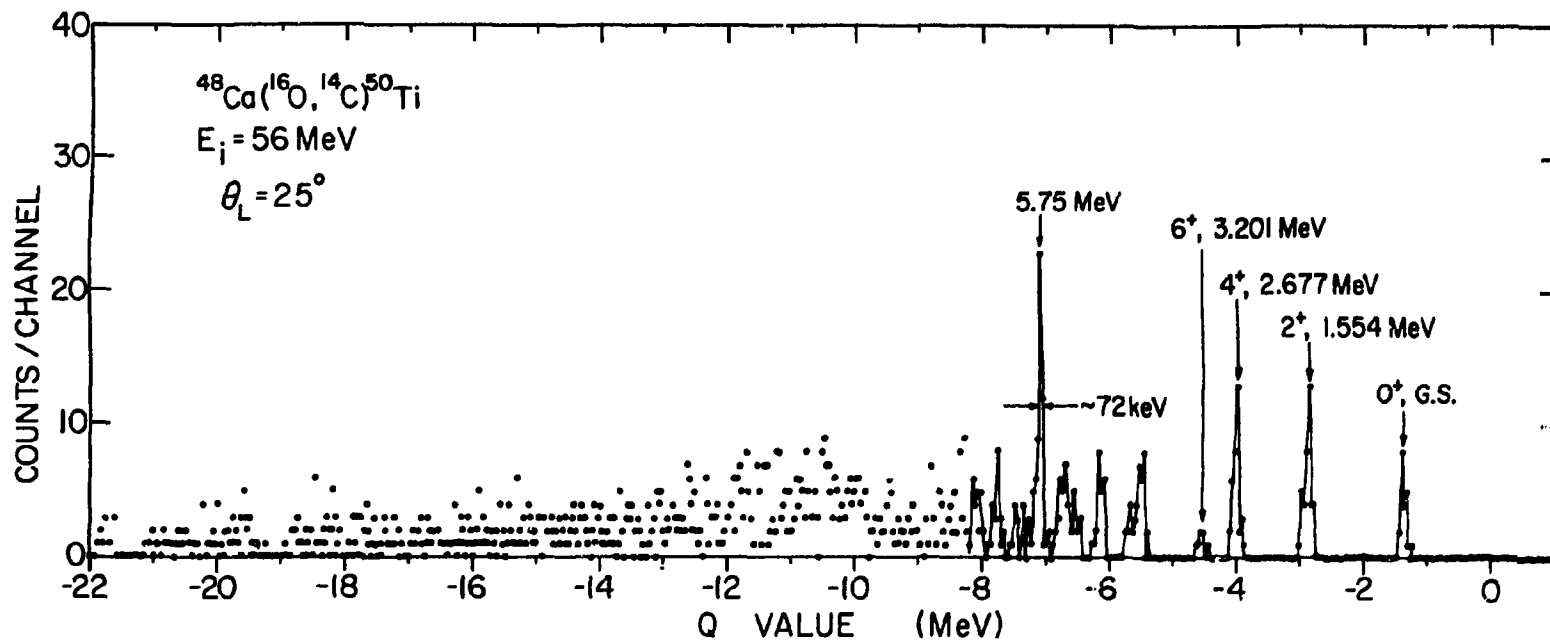
Fig. 8. An example of a $^{48}Ca(^{16}O,^{14}C)^{50}Ti$ spectrum. Note the zero background near the lower excited states. This spectrum covers 20 MeV excitation which corresponds to a 40% energy bite. The resolution is target limited (Ref. 8).
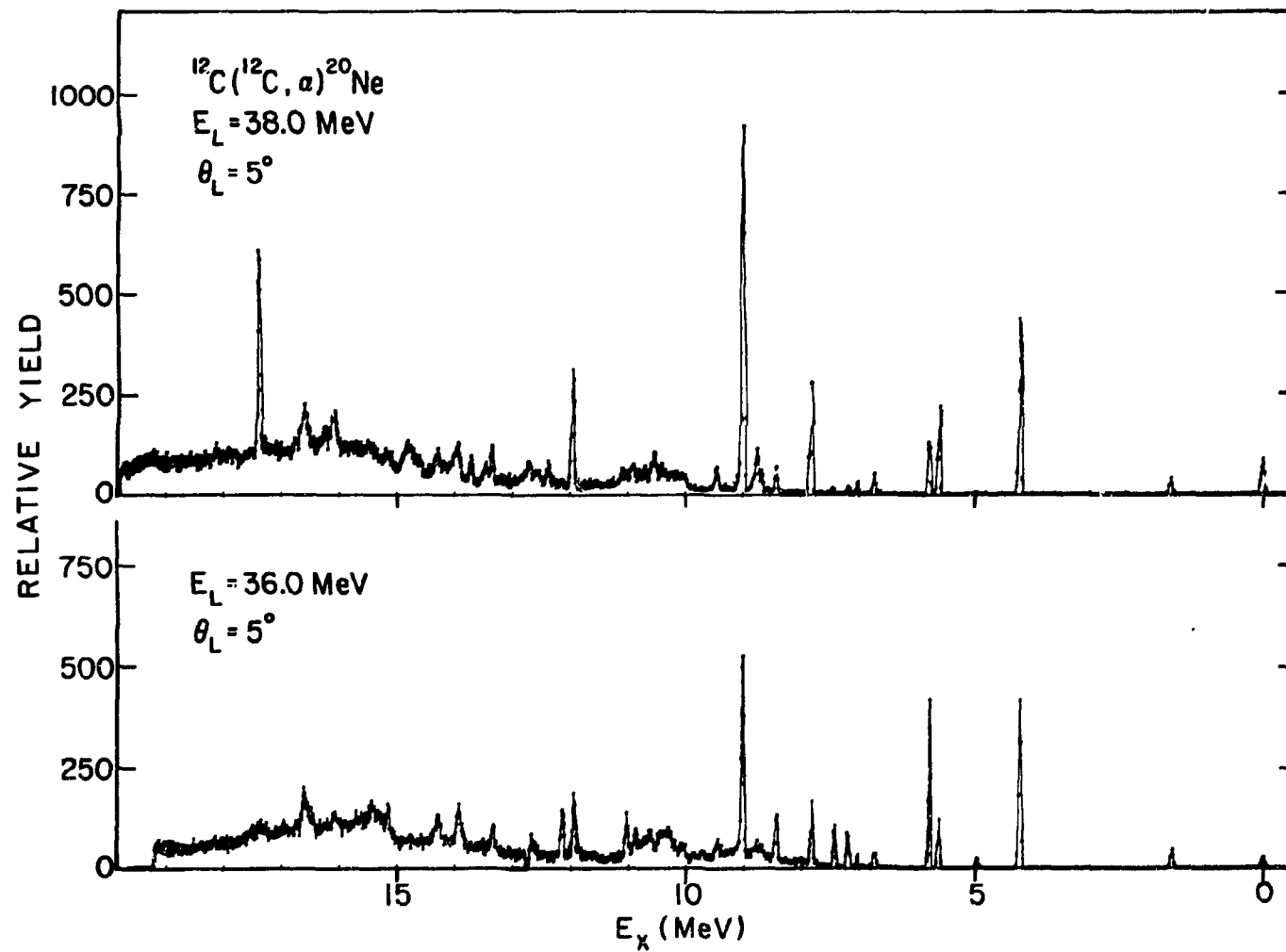
Fig. 9a. Spectra for the $^{12}C(^{12}C,\alpha)^{20}Ne$ reaction at θ_{lab} = 5° at $E_{lab}(^{12}C)$ = 36.0 and 38.0 MeV. Note the large fluctuation for individual levels from energy to energy (Ref. 20).
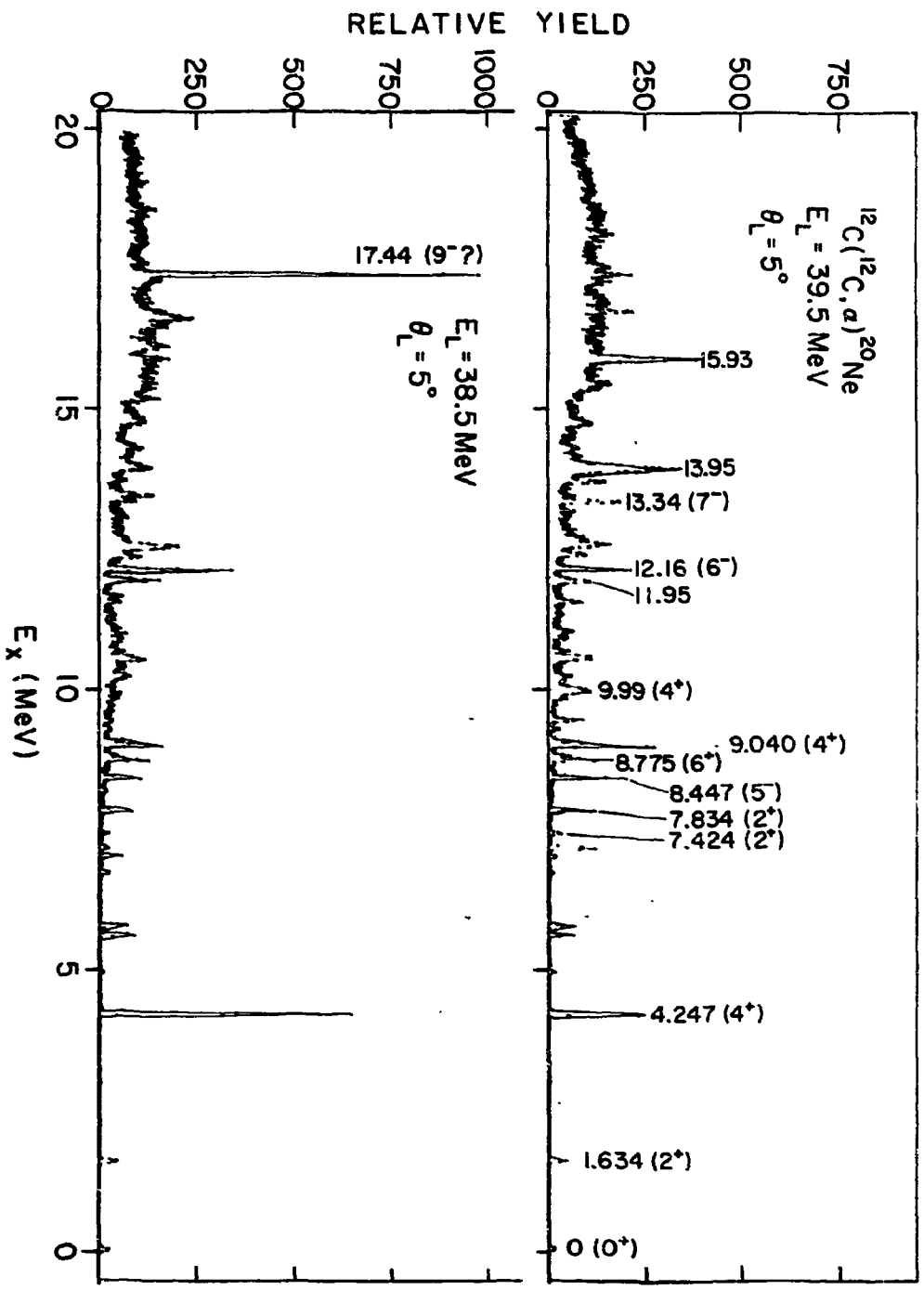
Fig. 9b. Spectra for the $^{12}C(^{12}C,\alpha)^{20}Ne$ reaction at θ_{lab} = 5° at $E_{lab}(^{12}C)$ = 38.5 and 39.5 MeV. Note the large fluctuation for individual levels from energy to energy (Ref. 20).

RELATIVE YIELD

$^{12}C(^{12}C,\alpha)^{20}Ne$
E_L = 39.5 MeV
θ_L = 5°

E_L = 38.5 MeV
θ_L = 5°

17.44 (9⁻?)

15.93

13.95

13.34 (7⁻)

12.16 (6⁻)
11.95

9.99 (4⁺)

9.040 (4⁺)
8.775 (6⁺)
8.447 (5⁻)
7.834 (2⁺)
7.424 (2⁺)

4.247 (4⁺)

1.634 (2⁺)

0 (0⁺)

E_x (MeV)
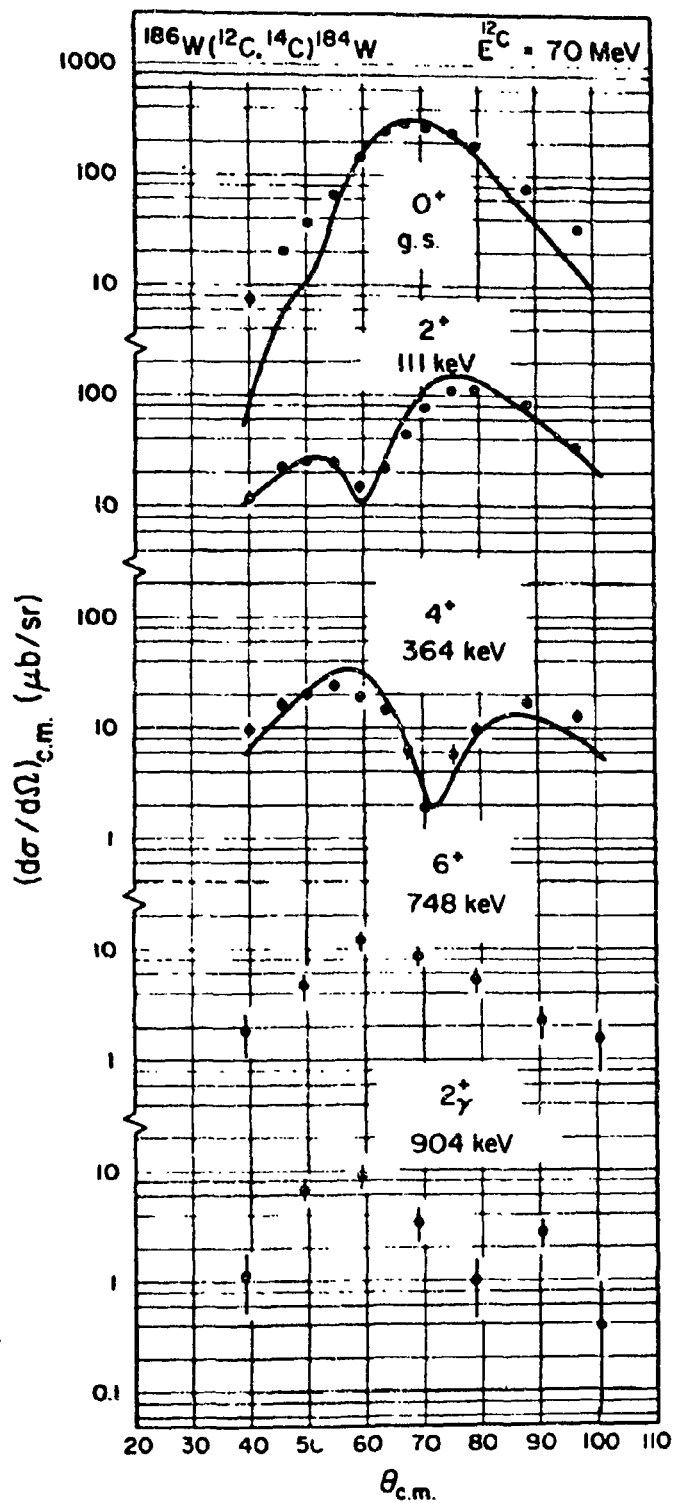
Fig. 10. Experimental and calculated (CCBA) angular distributions for the 0+, 2+, and 4+ members of the ground state rotational band in [184]W (Ref. 21).

[184]W as observed in the [186]W(^{12}C,[14]C) reaction[21] using the Brookhaven version of a Q3D spectrograph.[5] The broad minima found in the 2+ and 4+ data are due to interference between direct and indirect transitions. Reproducing this kind of data provides a sensitive test of our understanding of heavy ion reaction mechanisms.

G. **Nuclei Off the Stability Line.** Magnetic devices have long been used to detect nuclei off the line of stability. Energetic heavy ions make it possible to use reactions with very negative Q values and in which many nucleons are exchanged, thus increasing the number of rare isotopes which can be produced. A recent example is the use of the [208]Pb(^{18}O,[21]O) reaction by the Chalk River group to measure the mass excess of [21]O [Ref. 22]. A proportional counter backed by two 5 cm long position sensitive solid state counters was used at the focal plane of a Q3D spectrograph in order to identify and measure the energy of the particles. In Fig. 11 a two-dimensional plot of the ΔE signal from the proportional counter versus the E signal from one PSD measured with a solid angle of 1i msr shows the excellent separation obtained for [21]O[8+] ions. The observed [21]O spectrum was found to be consistent with the known level structure of the residual nucleus [205]Pb, thus supporting the identification of [21]O in this reaction. The properties of recoil mass spectrographs, and on-line isotope separators make them superior to a general purpose magnetic spectrograph for many investigations of very rare nuclei. However, the high energy resolution and large solid angle of a general purpose magnetic spectrograph makes it a useful supplement to other instruments for this type of research.

22
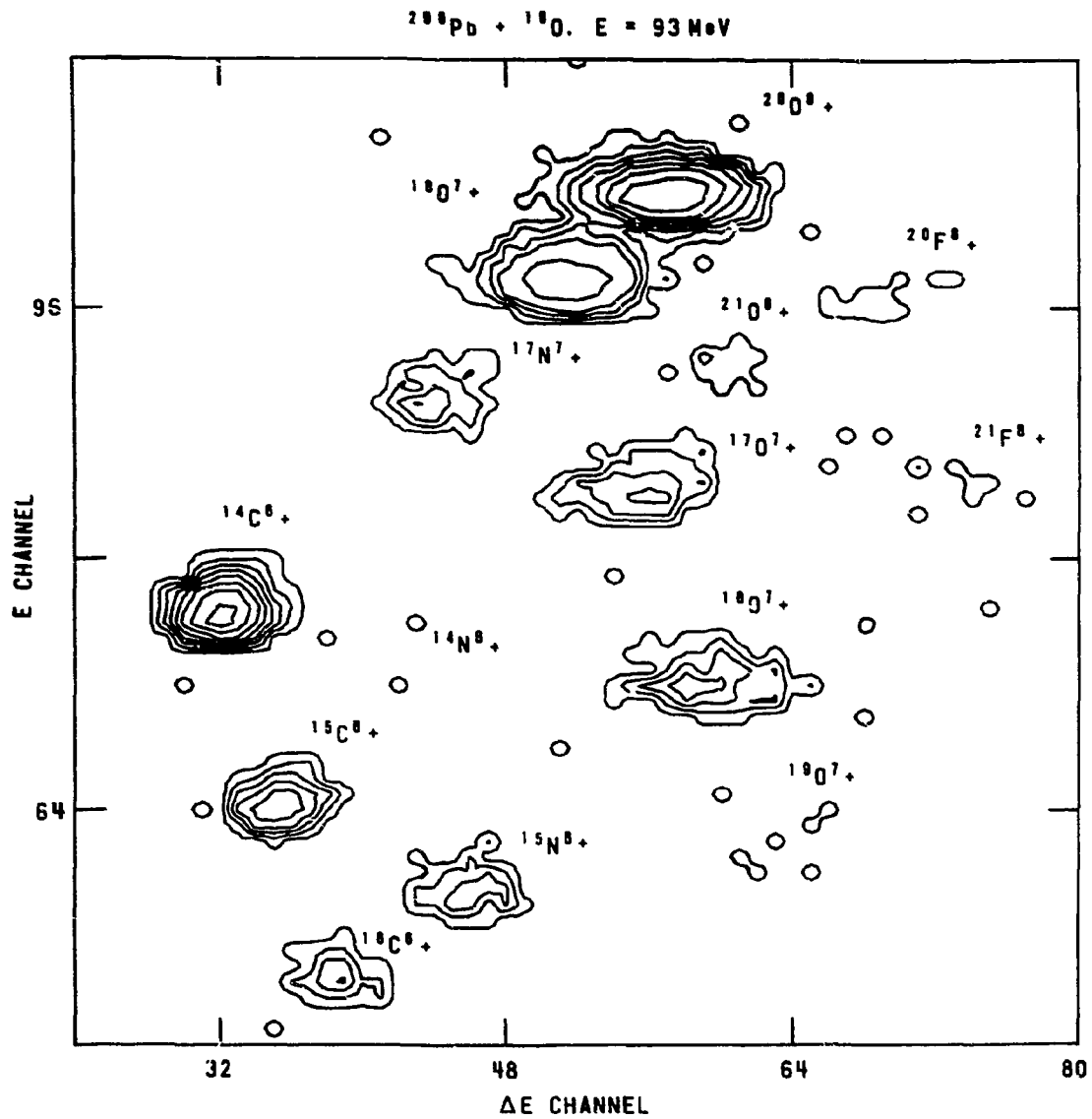
Fig. 11. A portion of the two-dimensional logarithmic contour plot of the ΔE proportional counter signal versus the E signal from a position sensitive detector centered on the $^{208}Pb(^{18}O,^{21}O)^{205}Pb$ ground state. The contours represent factors of two above the minimum value of one count (Ref. 22).

H. Coincidence Measurements. Particle-particle, and particle-gamma coincidence experiments are frequently necessary in order to measure the spins and decay modes of excited states in nuclei. Such measurements usually require that at least one of the particles be detected with high resolution. The high resolution, large solid angle and kinematic compensation possible with a magnetic spectrograph make it a superior instrument for such experiments.

As an example of such work the measurements on the $^{12}C(^{12}C,\alpha)$ reaction at the University of Pennsylvania can be cited.[23] There are states selectively populated in this reaction which decay neither by γ-emission nor by α-particle emission to a spin-zero state, but instead by α-particle emission to states with nonzero spin. In order to assign spins to such states a triple-angular correlation technique was used as illustrated in Fig. 12. The first α particle was observed at zero degrees relative to the beam direction by means of a magnetic spectrometer and the second α particle in a movable position sensitive solid state detector. Figure 13 demonstrates how clearly the spin can be established for a case in which the second α-particle decays to the ^{16}O ground state.

The above examples of the application of magnetic spectrographs are, of course, based on types of experiments which are already being conducted. Although such work will continue to be very important in heavy ion research, as research with heavier and more energetic ions progresses new effects and reaction mechanisms will appear. Possible properties of the nucleus such as viscosity, compressibility, and

$^{12}C + {}^{12}C \rightarrow {}^{20}Ne + \alpha_1$

$\phantom{^{12}C + {}^{12}C \rightarrow} \rightarrow {}^{16}O^* + \alpha_2$

$\phantom{^{12}C + {}^{12}C \rightarrow {}^{16}O^*} \rightarrow {}^{16}O(g.s.) + \gamma$

POSITION SENSITIVE
DETECTOR
(α_1)

SLICE
DETECTOR
(α_2)

^{12}C BEAM

^{12}C
TARGET

Na I(Tℓ)
(γ)

MAGNETIC
SPECTROMETER
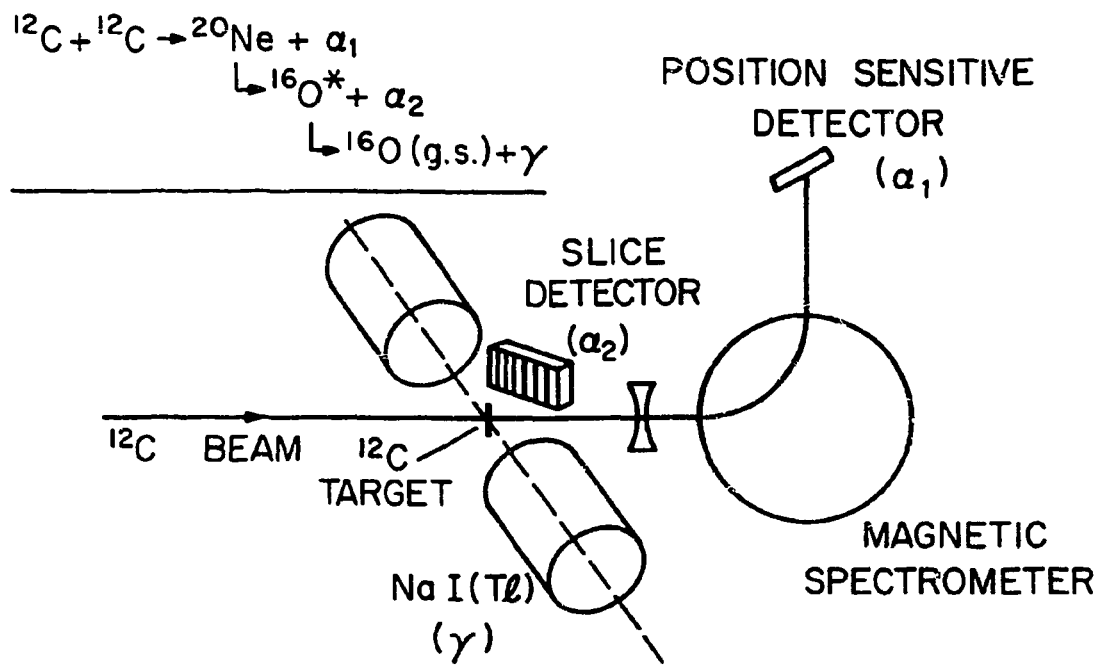
Fig. 12.   The experimental arrangement used in the triple correlation
measurements at the University of Pennsylvania (Ref. 23).
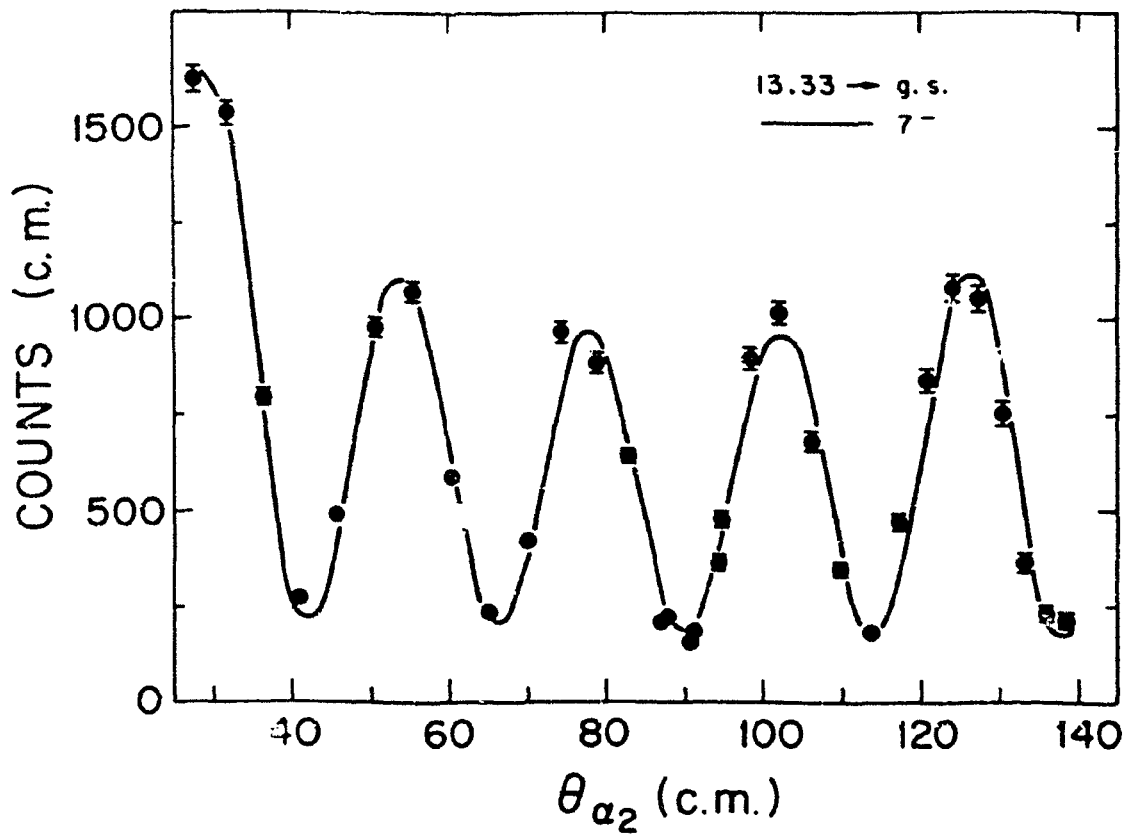
Fig. 13. Double (α_1 - α_2) correlation of the decays of the known 7⁻ state at 13.33 MeV in ^{20}Ne populated in the $^{12}C(^{12}C,\alpha)$ reaction to the ^{16}O ground state. The solid curve is the best fit to $[P_7 (\cos \theta)]^2$ + constant, integrated over the finite solid angle of the detector (Ref. 23).

superconducting effects will be investigated. Fusion reactions and deep inelastic scattering experiments indicate that new reaction modes remain to be explored. In many of these areas a magnetic spectrograph will help provide the detailed data necessary for a complete understanding of the processes involved.

IV. ENERGY RESOLUTION IN HEAVY ION REACTIONS
A. Limiting Factors in Heavy Ion Reactions

Although the examples of Section III make it clear that high resolution work with heavy ions is both valuable and feasible, the fact remains that the properties of heavy ions themselves definitely limit the resolution that can be achieved. High resolution work involves not only proper magnet design and proper beam handling, but perhaps most importantly extremely difficult target requirements. The preparation of proper targets will be crucial for high resolution, heavy ion experiments.

Limitations in high resolution work due to the target material include the following factors:

a) Energy loss straggling. Not all ions of a monoenergetic beam lose the same amount of energy in passing through a target foil. In the calculations to be discussed the energy spread due to energy loss straggling was estimated from the formula,

$$(\delta E)_{ES} = 30z \left[\frac{Z}{A} t \right]^{\frac{1}{2}} \text{ keV,} \qquad (1)$$

where Z and A are the atomic and mass numbers of the stopping material,

t its thickness in mg/cm^2, and z the equilibrium charge of the moving ion. The above expression is an approximation for the equation reported by Williams.[24] For heavy ions incident on very thin targets the energy spread due to straggling will approach the average energy loss in the target.

b) Target uniformity. As pointed out by Alonso and Harvey in their paper dealing with problems of high resolution heavy ion experiments a surface irregularity of only 20 atoms represents a target thickness variation of about 10 μgm/cm^2.[25] This irregularity already limits the obtainable resolution of a 5 MeV/nucleon Ar beam incident on a 50 μgm/cm^2 target to $\Delta E/E \geq 3 \times 10^{-4}$. The uniformity of thin targets then presents a major problem in heavy ion research.

c) Multiple scattering. A measure of the change in energy with scattering angle in a reaction is given by the parameter

$$k = \frac{1}{p} \frac{dp}{d\theta} .$$ (2)

Since a beam passing through a target experiences angular spreading due to multiple small angle Coulomb scattering, and since the energy of emitted particles in heavy ion reactions typically depends sensitively on the scattering angle, multiple scattering within the target introduces an energy uncertainty given by,

$$(\frac{\delta E}{E})_{MS} = 2 k \, \delta\theta_s ,$$ (3)

where $\delta\theta_s$ is the half-angle for multiple scattering and $(\frac{\delta E}{E})_{MS}$ the energy spread within this half angle. The values of $\delta\theta_s$ were calculated

from the expressions and values given by Sigmund and Winterbon[26] using the computer code SWIMS.[27] Figure 14 plots the value of the half-angle in which 60% of the scattered beam is contained versus the target mass for various target thicknesses and a 360 MeV ^{40}Ca beam. Expressions which approximate the multiple scattering, angle distribution with a Gaussian curve have been given, as for example by Jackson.[28] Such expressions indicate that the angle varies as $z \cdot 1/E\sqrt{A_s}$, where E and A_s are the incident energy, and mass number of the stopping material. The Sigmund and Winterbon results also show that essentially identical angles are obtained for any incident ion with the same energy per nucleon (E/A ≃ E/2z). However, these more exact calculations also show that for heavy ions and thin targets the distributions are not Gaussian in shape. Instead for a given incident ion, energy, and target thickness in $\mu gm/cm^2$, the distributions have constantly narrower widths accompanied by larger and longer tails at large angles as A_s is increased. Curves such as those shown in Fig. 14 will then not increase monotonically with A_s, as predicted by the Jackson expression, until a value of $\delta\theta$ is taken which corresponds to including 80 to 90% of the scattered beam. However, rather than taking such large values for $\delta\theta$, and therefore, perhaps overemphasizing the contribution due to multiple scattering, the values of $\delta\theta$ shown in Fig. 14 were used in the calculations.

As is seen from the figure $\delta\theta_s$ increases rapidly with target thickness, and multiple scattering will be a limiting factor for the resolution that can be obtained for very heavy ions from the new 25 MV tandem.
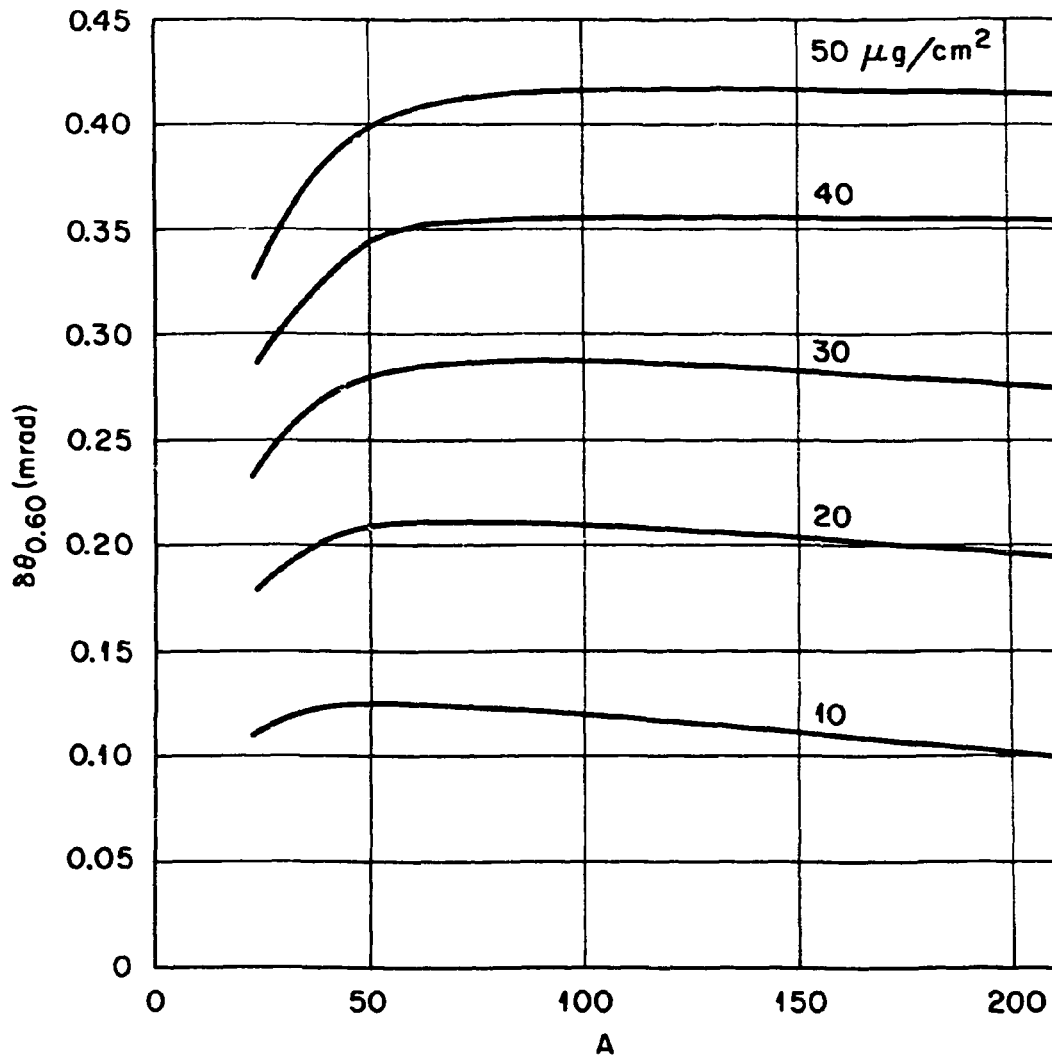
Fig. 14. Values of the multiple scattering half-angle contain-
ing 60% of the scattered beam plotted against the
target A value for various target thicknesses in
μgm/cm². The incident ions are for a 360 MeV ⁴⁰Ca
beam. The curves were calculated from the Sigmund-
Winterbon expression (Ref. 26) using the computer code
SWIMS (Ref. 27).

d) **Path length difference.** The energy of a reaction particle emerging

from a target foil will depend on the location within the foil of the

reaction site. Particles produced at different sites will have varying

energies since both the incident projectile and the reaction product will

traverse varying amounts of target material. These effects can sometimes

be corrected by a suitable orientation of the target angle,[13,29-31]

however, the angle required may often be too large to be practical. In

the present calculations the energy difference between reaction products

produced at the front and back of the target foil was taken as a measure

of the energy spread introduced by this effect.

To the above target sources of finite resolution must be added

those due to the finite emittance of the incident beam the effects of

which are coupled to the characteristics of the detection system. The

geometric beam emittance is given by,

$$\varepsilon = \pi\, x_o \cdot \theta_o \; , \tag{4}$$

where x_o and θ_o are the half widths of the spacial and angular dimensions

of the beam. The value of the beam emittance depends on the ion species,

type of terminal stripper, and configuration of the accelerator. Under

the assumption that gas stripping does not appreciably increase the

phase space area, the emittance for gas stripping at 25 MV in the new

tandem will be equal to, or less than,

$$\varepsilon = \frac{3.4\,\pi}{\sqrt{q + 1}} \quad \text{mm-mrad}, \tag{5}$$

where q is the charge state of the accelerated ion after stripping in

the terminal. Since the most probable charge state for gaseous stripping

of heavy ions at 25 MV is about 8, the emittance under these assumptions will have a maximum value of $\varepsilon = 3.56$ mm-mrad (it can also be much less). For comparison, the accelerator configuration limits the maximum emittance under all conditions (such as foil stripping in the terminal and in the high-energy accelerating tube) to 6π mm-mrad.[32] Since high resolution work will usually require the optimum accelerator conditions, and will primarily be performed with light-heavy ions (see Sect. IV.B) a full beam emittance of 2 mm-mrad was used in the calculations.

If the beam emittance is then approximated by the expression,

$$\varepsilon = x_T \cdot \theta_T \tag{6}$$

where x_T is the full width of the beam spot on the target and θ_T is the full angular spread of the beam, then the energy spread due to this angular spread is,

$$\left(\frac{\delta E}{E}\right)_{DIV} = 2k\theta_T = \frac{2k\varepsilon}{x_T} . \tag{7}$$

The size of the beam spot on the target also limits the resolution that can be obtained for a given spectrograph as given by the relation,

$$\left(\frac{E}{\delta E}\right)_t = \frac{DR}{2M_h x_T} . \tag{8}$$

The quantities D and M_h are the dispersion and horizontal magnification respectively, along the focal plane, and R is the radius of curvature in the magnet. These effects added in quadrature give,

$$\frac{\delta E}{E} = 2 \left[\left(\frac{M_h x_T}{DR}\right)^2 + \left(\frac{K\varepsilon}{x_T}\right)^2 \right]^{\frac{1}{2}} . \tag{9}$$

Figure 15 shows typical curves for the obtainable resolution calculated
for a split-pole spectrograph and various values of the kinematic shift
k, assuming that the beam emittance is 2 mm-mrad. These calculations
have also assumed that there is no contribution from the finite position
resolution of the focal-plane detector. In practice, however, the
detector places an upper limit on the resolution that can be achieved.
For example, a detector resolution of 0.5 mm together with the dispersion
of ∿ 2 for a standard split-pole spectrograph limits the energy resolution
to $E/\delta E \leq 2000$ (also see Sect. V.E).

If k is nonzero the curves in Fig. 15 have a maximum of

$$(\frac{E}{\delta E})_{max} = \left[\frac{DR}{8M_h k \varepsilon} \right]^{\frac{1}{2}} . \tag{10}$$

This is the upper limit, neglecting target and detector effects, for the
energy resolution that can be obtained for a given spectrograph and re-
action if the full emittance of the accelerator is utilized. Of course,
the value for $E/\delta E$ can be increased if slits are used to reduce the
beam emittance ε. It is also true that it is possible to correct for
the beam phase space volume by suitable beam transport techniques so
that the terms on the right hand size of Eqn. ∿ cancel (also see
Sect. IV.B).

The target effects a) through d) must finally then be added in
quadrature to determine the resolution that can be obtained in a
practical situation. Calculations based on the above formulae will be
discussed in the next section.

ORNL-DWG 76-11466
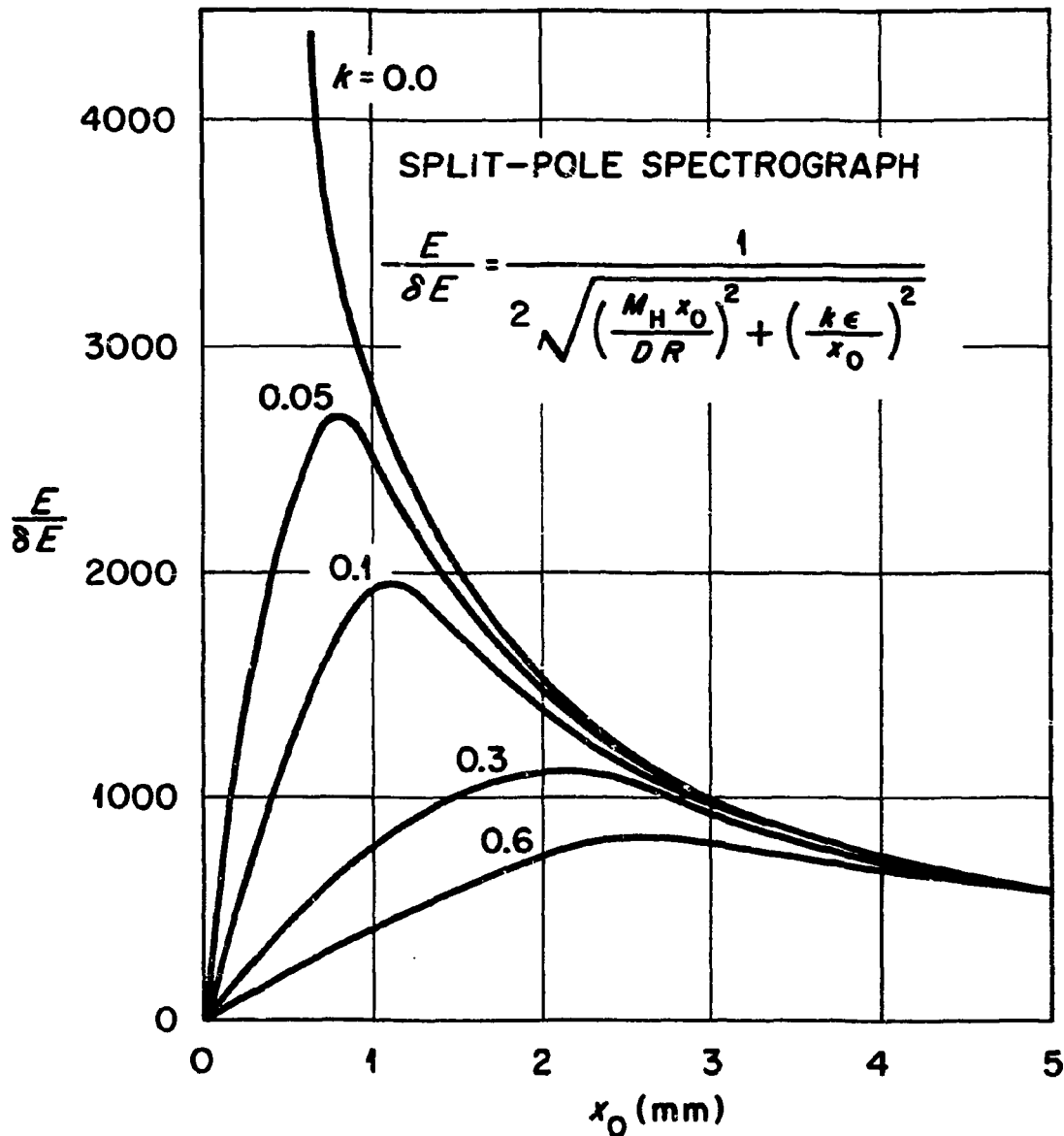
Fig. 15. Curves indicating the resolution attainable from a split pole
spectrograph (Ref. 15) due to limitations imposed by the kinetic effects
of the converging incident beam and finite beam spot on the target.
The parameters of the spectrograph were taken to be M_H = 0.34, D = 1.75m
and R = 1m. The quantity x_O is the full width of the beam spot on the
target. An emittance of 2 mm-mrad has been assumed. However, if for
example, the emittance is instead taken to be a factor of four larger,
then $(E/\delta E)_{max}$ is reduced by a factor of two, and x_O represents the
half width of the beam spot. Limitations due to target effects or the
detector resolution are not included.

B. Calculations

Figure 16 illustrates the ion energy performance as a function of ion mass for heavy ion beams available presently from ORIC, those expected from the 25 MV tandem accelerator, and those expected from the tandem + ORIC combination. The tandem curve is computed for a gas stripper in the terminal and foil stripping in the high-energy accelerating tube. The tandem + ORIC curve is computed for gas stripping in the terminal and foil stripping in ORIC. Both cases assume selection of the most probable charge state following each stripping so that both curves could be raised (at the cost of intensity) by going off the peaks of the charge state distribution. The dashed line marks the position of the Coulomb barrier for any of these ions on a lead target nucleus.

Table 1 lists the various contributions to the expected experimental resolution for a variety of targets and ions for incident energies with which it would appear feasible to do nuclear physics with the new tandem (see Fig. 16). The cases calculated are for (HI,α) reactions and elastic scattering at a laboratory angle of 20° since these examples are representative of situations where light or heavy ions are detected. Other than carbon, the target thickness was assumed to be either 50 $\mu gm/cm^2$ (self-supporting) or 10 $\mu gm/cm^2$ (with a 10 $\mu gm/cm^2$ thick carbon backing). The values shown for energy spreading due to straggling are those obtained by multiplying the results from Eqn. 1 by a factor of 1.6 in order to include the effect due to charge-exchange straggling,[33] although in cases this may overestimate the contributions due to straggling.[*] The

[*] This is only a crude estimate. Exact calculations by Pühlhofer[34] for charge-exchange straggling of heavy ions in gases yield values from about 5 to 13%.

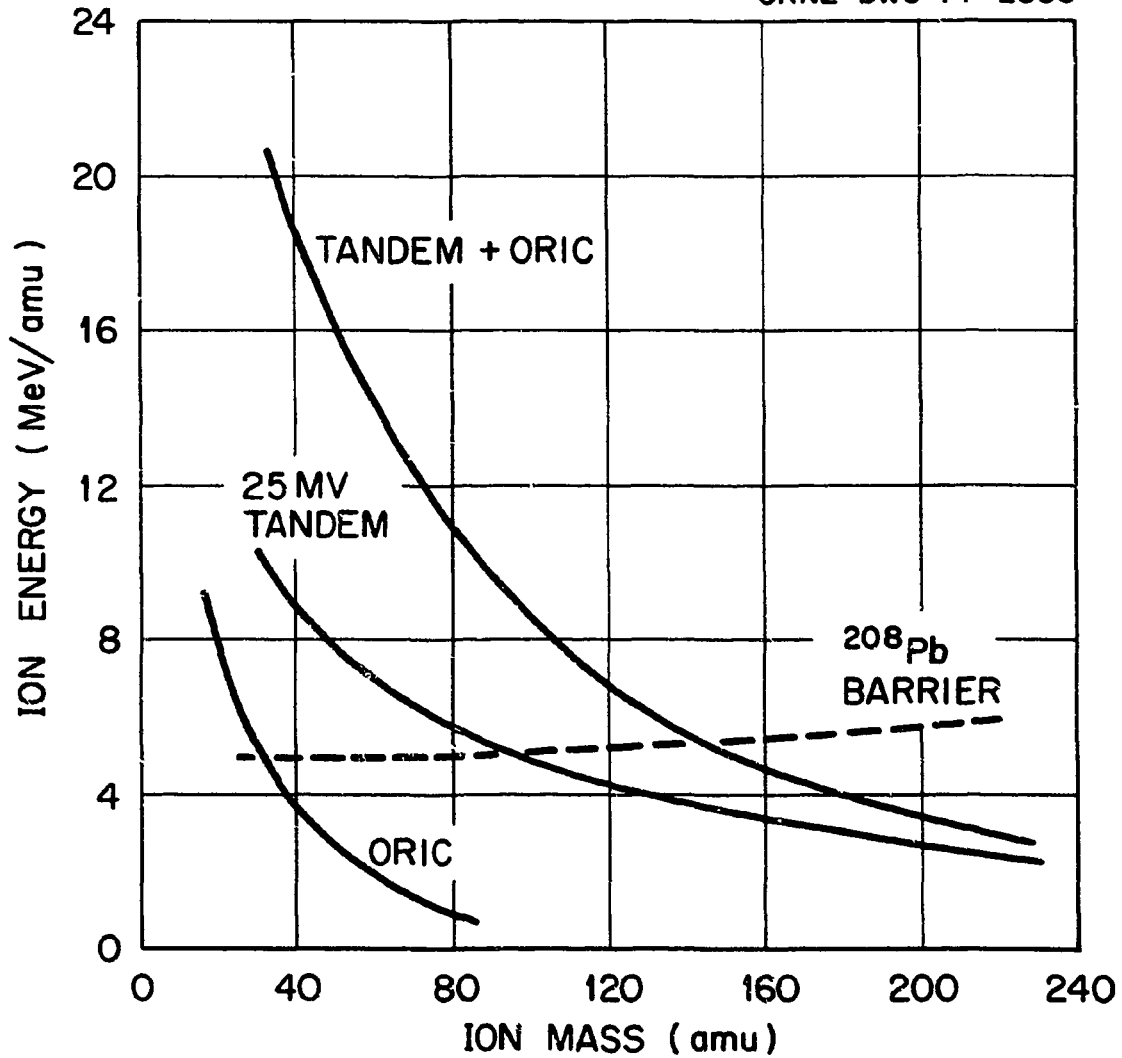Fig. 16. Beam energy as a function of ion mass for the separate and combined accelerators of the Holifield Heavy Ion Research Facility.

Table 1. Contributions to Finite Energy Resolution due to Target Thickness and a Split-Pole Spectrograph at 20° with Full Beam Emittance

Reaction	Energy (MeV)	Target Thickness (µgm/cm²)	Energy and Charge Straggling Target (keV)	Energy and Charge Straggling backing (keV)	Target Nonuniformities Target (keV)	Target Nonuniformities Backing (keV)	Effect of Path Length Difference (keV)	Multiple Scattering Target (keV)	Multiple Scattering Backing (keV)	Total Energy Spread due to Target (keV)	$(E/\delta E)_{max}$* due to Split-pole with full Beam Emittance at 20°	Total Energy Spread
^{12}C(^{12}C,^{12}C)	100	10	20		4		2	16		26	1000	103
	175	10	20		2		1	16		26	1000	180
^{12}C(^{12}C,α)	100	10	20		4		15	6		26	1570	65
	175	10	20		2		10	7		23	1555	110
^{24}Mg(^{12}C,^{12}C)	100	10 on 10C	20	20	3	4	1	9	16	34	1450	80
	175	10 on 10C	20	20	2	2		16	16	36	1450	125
^{24}Mg(^{12}C,α)	100	10 on 10C	20	20	3	4	13	4	16	36	2130	60
	175	10 on 10C	20	20	2	2	8	4	16	34	2100	85
^{58}Ni(^{12}C,^{12}C)	100	10 on 10C	20	20	3	4		5	16	33	2140	60
	175	10 on 10C	20	20	2	2		5	16	33	2140	85
	175	50	45		8			15		48	2140	95
^{58}Ni(^{12}C,α)	175	10 on 10C	20	20	2	2	8	3	16	34	3078	70
	175	50	45		8		39	4		60	3078	85
^{120}Sn(^{12}C,^{12}C)	100	10 on 10C	19	20	2	4		2	16	32	3264	45
	175	10 on 10C	19	20	2	2		2	16	32	3264	60
	175	50	42		8			6		43	3264	65
^{120}Sn(^{12}C,α)	175	10 on 10C	19	20	2	2	8	1	16	33	4340	50
	175	50	42		8		40	4		58	4340	70
^{58}Ni(^{28}Si,^{28}Si)	225	50	104		27			73		130	1450	205
^{107}Ag(^{40}Ca,^{40}Ca)	375	10 on 10C	64	68	14	25		24	100	143	1610	270
	375	50	142		35			86		169	1610	285
^{153}Eu(^{40}Ca,^{40}Ca)	180	50	138			32		27		145	2016	170
	360	50	138			35		55		152	2016	235
^{197}Au(^{58}Ni,^{58}Ni)	200	50	190			50		42		203	1900	230
	400	50	190			60		84		214	1900	300
^{197}Au(^{90}Zr,^{90}Zr)	225	50	271			87		92		300	1520	330
	450	50	271			90		184		340	1520	450

*The contributions of the spectrograph due to the beam phase space volume can be reduced by suitable beam transport techniques.

36

contribution due to target non-uniformities was taken to be 10% of the energy loss in the target for 50 $\mu gm/cm^2$ thick targets, and 20% of the energy loss for 10 $\mu gm/cm^2$ thick targets. The contributions due to a spectrograph are those for a split-pole magnet and a beam emittance of 2 mm-mrad (see Fig. 15).

It is clear from Table 1 that high resolution spectroscopy is feasible with the energetic, light-heavy ions (i.e. $^{10,11}B$, $^{12,13}C$, ^{14}N, ^{16}O) available from the 25 MV tandem. Target effects, dominated by straggling and multiple scattering, still permit a value for the resolution $E/\Delta E$, of at least 2000 to 3000. The contribution due to the finite energy spread of the incident beam must still be added; however, the energy stability of $\pm$ 0.05% ($E/\Delta E$ = 2000) or better specified for the new tandem[35] should allow the experimental resolution to be 0.1% or better. The contribution of the energy spread in the incident beam of the cyclotron may be larger.

The last column in Table 1 includes the contribution due to a split-pole spectrograph[15] assuming a beam emittance of 2 mm-mrad, a scattering angle of 20°, and a spectrograph resolution $(E/\delta E)_{max}$ corresponding to Eqn. 9 (the maxima of the curves shown in Fig. 15). It is seen that $(E/\delta E)_t$ then varies from about 970 to 3300 for the light-heavy ions. Of course, the contribution of the spectrograph can be reduced by either utilizing a smaller portion of the incident beam emittance, or by measuring the data at a smaller laboratory angle. It should be noted that most of the available high resolution (HI,α) measurements have been performed at laboratory angles between 5 and 10°.

Magnetic spectrographs also make it possible to reduce the effects of finite beam emittance without reducing the emittance by locating the position of the beam focus on a point other than the target.[36]

As the mass of the incident projectile is increased, the contributions due to straggling and target non-uniformities increase and rapidly limit the energy resolution feasible for even the thinnest practical self-supporting targets (about 50 $\mu gm/cm^2$ for most materials). If instead the targets are placed on carbon backings, then multiple scattering, particularly in the carbon backing, becomes the limitation. This is particular true for the heavier ions where the energies will be less than or equal to 5 MeV/nucleon from the new machine (see Fig. 16). The relative importance of straggling and multiple scattering for such ions is well illustrated in Table 2 taken from the paper of Alonso and Harvey.[25]

The contribution due to multiple scattering in 10 $\mu gm/cm^2$ thick carbon foils is about 100 keV for 375 MeV ^{40}Ca ions. Therefore, if a resolution of about 100 keV is taken to be the upper limit for detailed nuclear spectroscopy such work should be possible with the new tandem for heavy ions with masses up to about 28, and in some circumstances up to mass 40. It is also true that in addition to the energy resolution problems, the identification of ions heavier than about A=60 becomes more difficult since the reaction products are produced in various charge states which begin to overlap. Therefore, the number of parameters which are measured (and with good resolution) must be increased.

It should be noted, however, that the usefulness of magnetic spectrographs is not limited to situations in which high energy resolution

Table 2

Maximum Gold Target Thickness (ug/cm^2) to Keep Energy Dispersive Effects
to within 0.03%

(The number in columns A and B give the contributions only from the effect
named at the top of the column.)

Beam	A Straggling	B Multiple Scattering at $\theta_{lab} = 20^o$	
		Au	Au + Backing
C	22	3800	3800
Ar	35	340	340
Kr	80	63	55
Xe	125	21	15
U	170	4	--*

*Best possible resolution for solid target is 5×10^{-4}, for zero gold
thickness (caused entirely by scattering in carbon backing).

can be obtained. The large solid angle, high background suppression,
zero-degree capabilities and freedom from radiation damage make a magnet
advantageous for many types of experiments where the modest energy re-
solution available from other types of detectors would be sufficient.
Examples include reaction mechanism studies where observation of the
ground state and at most the first few excited states may be enough to
establish the nature of the reaction, and detection of rare nuclei. No
matter what the experimental situation or limitations, the energy
resolution that can be obtained from a magnetic spectrograph is equal
to or superior to that obtainable from other types of detection apparatus.
Above all the superb particle identification ability of a spectrograph,
when operated with modern focal plane detectors, makes such a system
unmatched for analyzing many types of heavy ion reactions.

V. DESIRABLE CHARACTERISTICS OF A HEAVY ION SPECTROGRAPH

In view of the characteristics of the 25 MV tandem and the ORIC
cyclotron and the energy resolution limitations discussed in Sect. IV,
the following properties appear desirable for the new spectrograph:

A. Energy Resolution. Since the incident ions will have energies up
to about 300 MeV, and an energy resolution of at least 100 keV is
desirable, the spectrograph should have a resolving power $(\delta E/E)$ of at
least 1/3000. Calculation of target and beam effects which can degrade
the resolution indicate that this resolving power will be useful for ions
at least as heavy as silicon.

B. Solid Angle. The maximum solid angle should be at least 20 msr.
In general in a magnet design one must trade off solid angle for im-
proved resolution. But new focal plane detectors[8,11,12] now make it
possible to correct for aberrations and incompletely corrected kinematic
shifts due to a large $\Delta\theta$ value, and, therefore, achieve good resolution
along with a very large solid angle.

C. Mass-Energy Product. For scattering and few-nucleon transfer
processes the reaction products are similar to the incident ion. High
resolution work with the tandem will probably be limited to projectiles
with A $\leq$ 40, and for these E/A $\leq$ 15. The relation for the mass-energy
product then gives

$$\frac{ME}{q^2} = (\frac{A}{q})^2 \; \frac{E}{A} \leq 60,$$

since $\frac{A}{q} \sim \frac{A}{Z} \sim 2$.

If one wishes to detect the compound nuclei, or evaporation residues
from fusion reactions instead, then,[37]

$$\frac{E_{CN}}{A_{CN}} = (A_{proj.}/(A_{proj.} + A_{target}))^2 \cdot E_{proj.}/A_{proj.}$$

$$\approx (\tfrac{1}{2})^2 \cdot (2.5 - 20) = (0.6 - 5) \; \text{MeV/nucleon.}$$

Consider, for example, a ^{16}O beam from the tandem plus ORIC combination
with E/A = 20 MeV/nucleon used to produce evaporation residues near
mass 120. Then the energy of the residues is about 600 MeV. The
average equilibrium charge state of 600 MeV ^{127}I ions is about 38
[Ref. 38] so that the required mass energy product is then 53. Over
the range of energies possible with either the tandem or the coupled

accelerators an EM/q^2 value between 20 and 60 is suitable for most heavy fusion products. Therefore, a magnet with a mass-energy product of 100 should be adequate for such experiments.

However, the energy of light ions emitted in energetic heavy ion collisions can be very similar to the energy of the projectile. The 90° analyzing magnet of the 25 MV tandem will have a mass-energy product of 320 and the cyclotron constant k, in the equation $E = k\,q^2/A$, is about 90 for ORIC. Therefore, a new spectrograph should have a mass-energy product of at least 200 in order to analyze both light and heavy ion reaction products from either the tandem or cyclotron.

D. **Kinematic Compensation.** As seen in Section IV the large kinematic energy shift due to center-of-mass motion in heavy ion reactions is one important source of finite resolution. The kinematic shift over the finite spread in the entrance angles accepted by a spectrograph are usually compensated for by either moving the focal plane,[39] or by changing the fields in a multipole element as in a Q3D spectrograph[6] provided the values of the kinematic shift factor k are not too large. However, recently developed focal plane detectors (e.g. Ref. 11) can determine particle trajectories so that a spectrum corresponding to the proper focal plane position can be constructed by computer techniques for many outgoing channels with very different kinematic shifts even though the counter remains fixed in position.

Figure 17 shows the values for k for elastic scattering for which M_T/M_i = 1,2,3,6, since for elastic scattering k depends only on this ratio. For comparison the curve for the ground state transition of
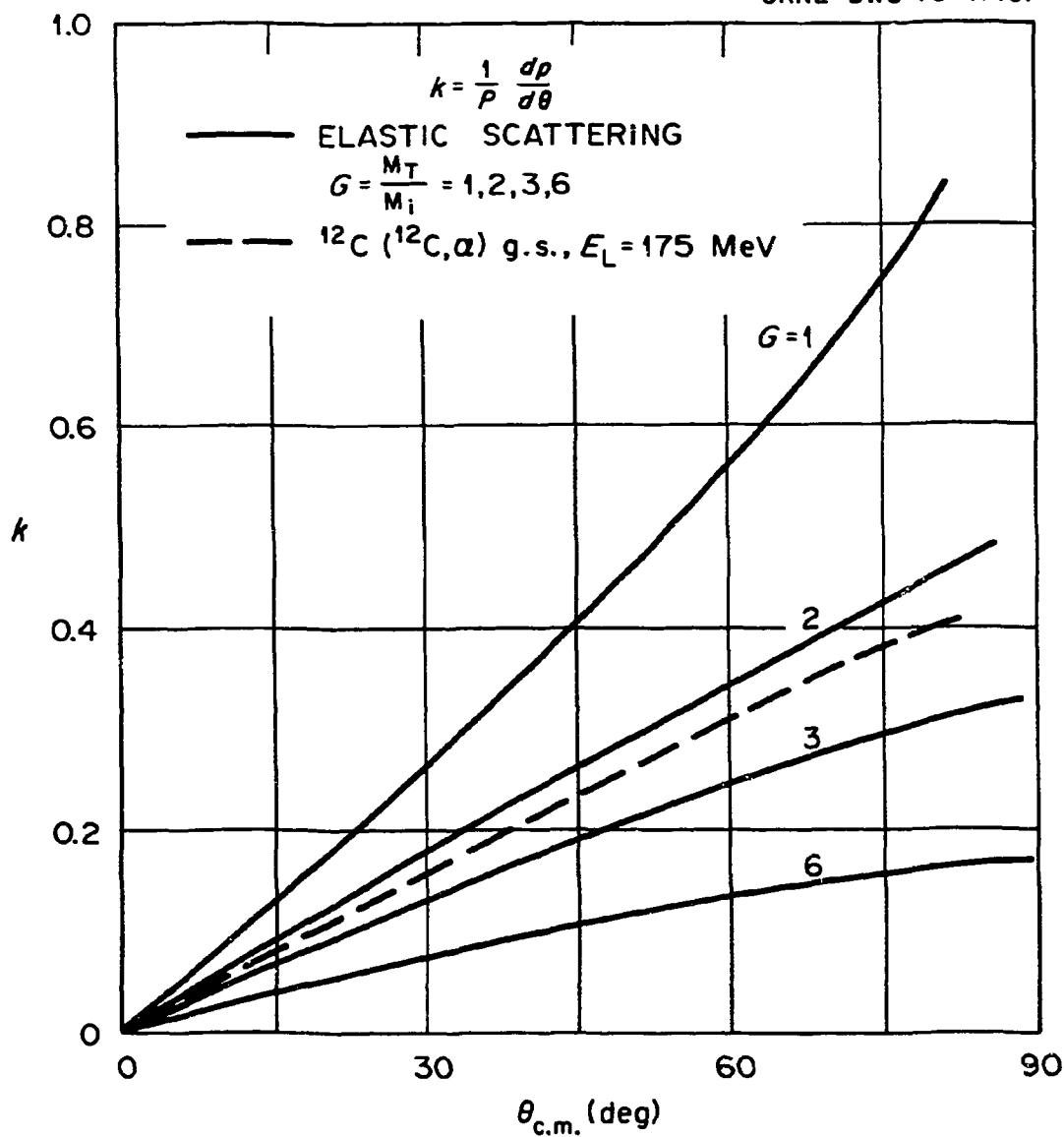
Fig. 17. The kinematic shift k as a function of scattering angle for elastic scattering for different values of the ratio of the target to projectile mass ($G = M_T/M_i$). The kinematic shift for the ground state transition of the $^{12}C(^{12}C,\alpha)$ reaction at 175 MeV is also shown for comparison.

the $^{12}C(^{12}C,\alpha)$ reaction at 175 MeV is also shown. At center-of-mass angles less than 45° the value of k is less than 0.5. It is easy to find heavy ion reactions with much larger values of k, particularly when there are an exchange of a number of nucleons. The $^{40}Ca(^{40}Ar,^{40}Ca)$ reaction, which could be considered a reaction in which the projectile picks up two protons and loses two neutrons, results in a ground state k value of 0.84 for an angle of 80° (c.m.) and an incident energy of 375 MeV. However, the grazing angle for this reaction is around 15° to 20° where the value of k is 0.18 or less.

Existing magnetic spectrographs can correct for kinematic shifts up to values of about 0.3. The version of the Q3D spectrograph planned for the Hahn-Meitner Institute in Berlin will permit corrections up to k = 0.5.[40] On the other hand, the magnet to be installed at the GSI will be suitable for kinematic shifts as large as 2.[41] However, the high resolution capabilities of the new tandem, together with the fact that many heavy ion reactions have peak cross sections near the grazing angle which are usually at small angles, imply that most of the measurements will be made at forward angles. Therefore, a maximum kinematic correction of k = 0.5 should be adequate.

E. Dispersion and Energy Range. The dispersion of the magnet should be suited to the position resolution of active focal plane detectors. It may be possible to build detectors for heavy ions that have a position resolution which is as good as 0.5 mm, but a safer and more conservative assumption would be a 1 mm position resolution for heavy ions. If the position resolution is 1 mm then a dispersion, D of about 8m (8 cm/%p) would be appropriate since this value corresponds to 0.25 keV/mm-MeV. A position resolution of 1 mm would then give an energy resolution of 25

keV/mm for 100 MeV particles. It would be very valuable if the dispersion were variable, varying from about 0.1 to 1 keV/mm-MeV, since then a wide range of reaction products can be first scanned with the low dispersion mode, and then the more interesting or higher cross section processes studied using the high resolution mode. Although, the GSI magnet[41] will have this feature, variable dispersion in general is hard to obtain in a magnet design, and it is expensive.

The energy range accepted by the spectrograph at a single magnetic field setting should be about 30% since this value should be adequate for collection of most of the charge states of detected heavy ions. This energy bite together with a dispersion of 8m will then require that the focal plane and detector be at least 1.2m in length.

In designing a magnet it is usually necessary to compromise when choosing the values for the dispersion and energy bite of a spectrograph since it is difficult to simultaneously have both large. However, a large energy bite is important in heavy ion reactions because of the presence of multiple charge states and the desirability of observing isolated states as well as continuum effects at high excitation energies. In addition a large value for the dispersion requires a larger focal plane motion for kinematic compensation since the amount of correction is roughly proportional to D x M (e.g. Ref. 36), and tends to reduce the angular magnification (see Sect. VG).

If the dispersion of the magnet is reduced from 8 to 4 m (0.50 keV/mm-MeV) then only a 60 cm long focal plane would be needed to give a 30% energy bite. This decreased focal plane length greatly simplifies the design and construction of the sophisticated, multi-parameter counters required for heavy ion detection. However, a focal plane detector with a position resolution of 0.5 mm would then be required in order to have 25

keV energy resolution for 100 MeV ions. Recent progress toward building
such detectors has been both rapid and encouraging (e.g. Refs. 42 and 43).
If heavy ion counters with submillimeter position resolution can be built
then the dispersion can be less and the spectrograph design simplified so
that a much wider choice of different magnet designs would be suitable for
the new facility.

F. <u>Vertical Magnification</u>. The problem of building active focal plane de-
tectors is greatly simplified if the image of the beam spot at the focal
plane is no larger than 1 cm. Therefore, the vertical magnification should
be less than or equal to three.

G. <u>Angular Magnification</u>. It is important to be able to measure the angle
at which a particle enters the spectrograph by means of focal plane de-
tectors which determine the particle trajectories (e.g. Refs. 8,11,12).
This information then makes it possible to measure the structure in an
angular distribution over the angles subtended by the spectrograph opening,
and to correct time-of-flight data for the nonisochronous orbits within
the magnet. However, the accuracy of ray tracing measurements is increased
if the angular magnification of the magnet is $\geq$ 2.

H. <u>Straight Focal Plane</u>. It is obvious that the focal plane detector is
an integral and critical part of a heavy ion spectrograph system. Therefore,
the focal plane should be straight to facilitate the design and use of
active counters. Ideally the angle at which particles strike the detector
should be normal in order to reduce multiple scattering effects which de-
grade the energy and energy-loss measurements in the case of non-normal
incidence. However, it is generally difficult in a magnet design to rotate
the particle rays so that they are normal to the focal plane while the same
time correcting for aberrations. The result often reduces the energy range
and deteriorates the vertical focussing of the instrument. The importance

of normal incidence may be reduced by detector designs which are either configurated to account for non normal incidence,[43,44] or which measure the position twice thus allowing the detector to be oriented so that the particles are normal to its face.[8,11,12]

I. Other Requirements. It should be possible to measure data at any scattering angle between -10° and 160°. The vacuum within the spectrograph should be of the order of 10^{-7} Torr to avoid serious loss of reaction products and a contribution to background counts due to charge change within the magnet.

IV. COMPARISON OF EXISTING AND PROPOSED SPECTROGRAPHS

Unfortunately a spectrograph with the ideal characteristics discussed in Sect. V does not presently exist. Table 3 lists the properties of some existing and proposed spectrographs.

The first entry in Table 3 is for the modification of the Elbek spectrograph[17,18] located at the ORIC cyclotron. A quadrupole magnet has been added between the scattering chamber and spectrograph entrance to increase the available solid angle thus producing a Q1D spectrograph.[45] This magnet then has an average solid angle of 5 msr (10 msr at the high energy end of the focal plane), and a mass-energy product of 210. It has a broad energy range (4.4) and good time-of-flight capabilities due to its large radius. However, since the particles strike the focal plane at the very oblique angle of 36°, and the dispersion is only 2 corresponding to 100 keV/mm for 100 MeV incident ions, while in addition the vertical magnification is 8, this magnet is not well suited to active focal plane detectors.

Table 3
Properties of Existing and Proposed Broad Range Spectrographs

	Oak Ridge Elbek plus Quadrupole QID	Oak Ridge-Argonne etc. Split-Pole	Berkeley QSD	Brookhaven QDMDD	Groningen QMDMDD	Berlin QMDMDD	Julich QQDMDQ	GSI QQDSQ	Indiana QDMDM	QSP	QSP-N
Range - E_{max}/E_{min}	4.4	8	1.30	1.51	1.20	1.20	1.10	1.17 - 1.66	1.015	3.5	2.2
Dispersion	2	1.75	4	6 - 11.5	8.1	6.8	16.9	5.3 - 1.4	15	2.1	2.1
Hor. Mag. - M_H	0.8	0.34	0.4	0.78 - 1.36	0.9	0.9	0.85	0.9	<1	0.30	0.30
D/M_H	2.5	5.1	10	7.5 - 8.5	9	7.2	19.85	5.9	~15	7	7
Vert. Mag. - M_V	4-8	3	5	3	6	6	7.2	2	~1	4.5	4.5
Solid Angle - msr	~5	3	2	14.7	10	10	10	3	4.8	8	8
Mass-Energy Product	200	90	315	121	193	140	540	450	250		
Kin. Corr.	Focal Plane	Focal Plane	Focal Plane	Multipole	Multipole	Multipole	Multipole	Quadrupole	Multipole	Focal Plane	Focal Plane

49

The second entry in Table 3 is for the version of the split-pole spectrograph[15] presently at the ORNL EN tandem. The solid angle listed for this spectrograph is the usual figure at which aberrations are not important. However, the new developments in focal plane detectors permitting ray tracing make it feasible to operate with very large solid angles by correcting for aberrations by computer after determining the path of each particle.[8,11] For example, data has been accumulated with the University of Rochester split-pole magnet utilizing a solid angle of 10 msr.[46] The ORNL split-pole still has the limitations that its mass-energy product is barely adequate for the new tandem and its dispersion is too small to be well matched to focal plane detectors.

These two existing spectrographs would together provide a reasonably satisfactory interim solution to the need for a spectrograph at the heavy ion facility while the design and procurement of a new generation spectrograph were proceeding. The superior qualities, such as solid angle and dispersion, of other spectrographs shown in Table 3 make a new magnet highly desireable.

Figure 18 displays a proposed layout for the new facility. The existing Elbek spectrograph is shown with beam lines making it accessible from both the cyclotron and new tandem. The existing split-pole is shown where it might be sited in one of the two scattering rooms of the 25 MV tandem. A new spectrograph could replace the Elbek magnet where there is available space to accommodate a spectrograph with overall radius up to at least 5.6 meters.
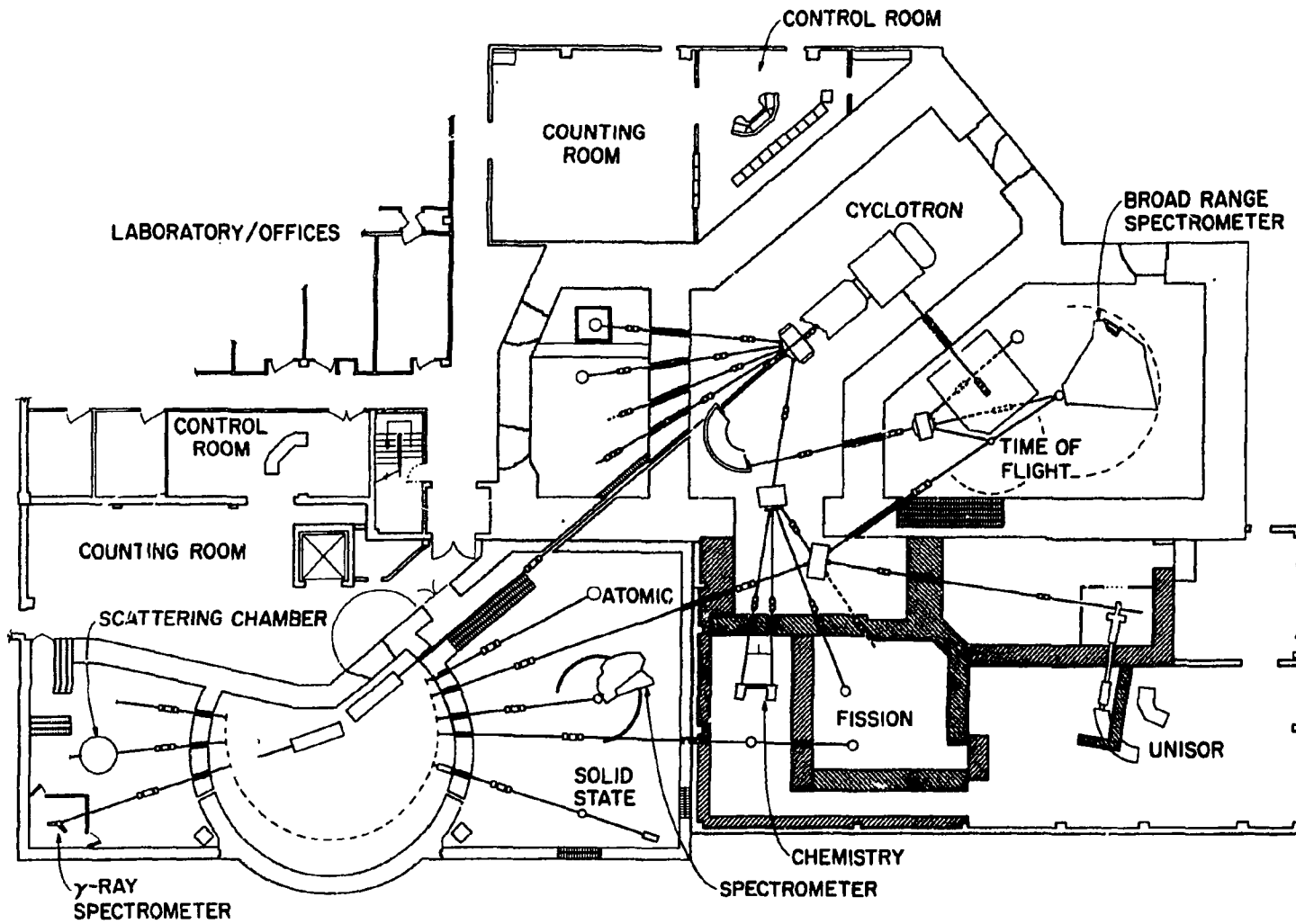
Fig. 18. Conceptual layout of the heavy ion laboratory beam lines and experimental equipment.

The other spectrographs in Table 3 include those planned for the
heavy ion facilities at the Hahn Meitner Institute in Berlin[40] and the
GSI,[41] and the very high resolution, large solid angle instrument
intended for light ion work at the Jülich cyclotron.[47] The last two
spectrographs listed are two proposed designs[48] by Enge to be discussed
in Sect. VII.

VII. POSSIBLE NEW SPECTROGRAPH DESIGNS

This section will briefly discuss some possible solutions to the
need for a new spectrograph. The actual design of such an instrument
must be studied and decided after the decision has been made that a
new spectrograph is a high priority device for the heavy ion facility.
Since two spectrographs exist which can initially be used with the new
accelerator, the study and design of a new spectrograph can be done
with the care and deliberation that such a large and costly instrument
deserves.

a) The Berkeley spectrograph has many desirable features; high
resolution for large kinematic shifts, reasonable dispersion, normal
incidence to the focal plane, and a large mass-energy product for its
weight and, therefore, cost. A new version of this spectrograph can
probably be designed with a solid angle of about 20 msr.[12] The
existing QSD spectrograph is shown in Fig. 19.

b) The version of the Q3D spectrograph under construction at
Groningen[49] (see Fig. 20) is very similar to that planned for the HMI,
Berlin except that the mass-energy product is 193 and the dispersion
8.1. Such a spectrograph would be an excellent instrument for the high
resolution work possible with incident ions up to about silicon, and will
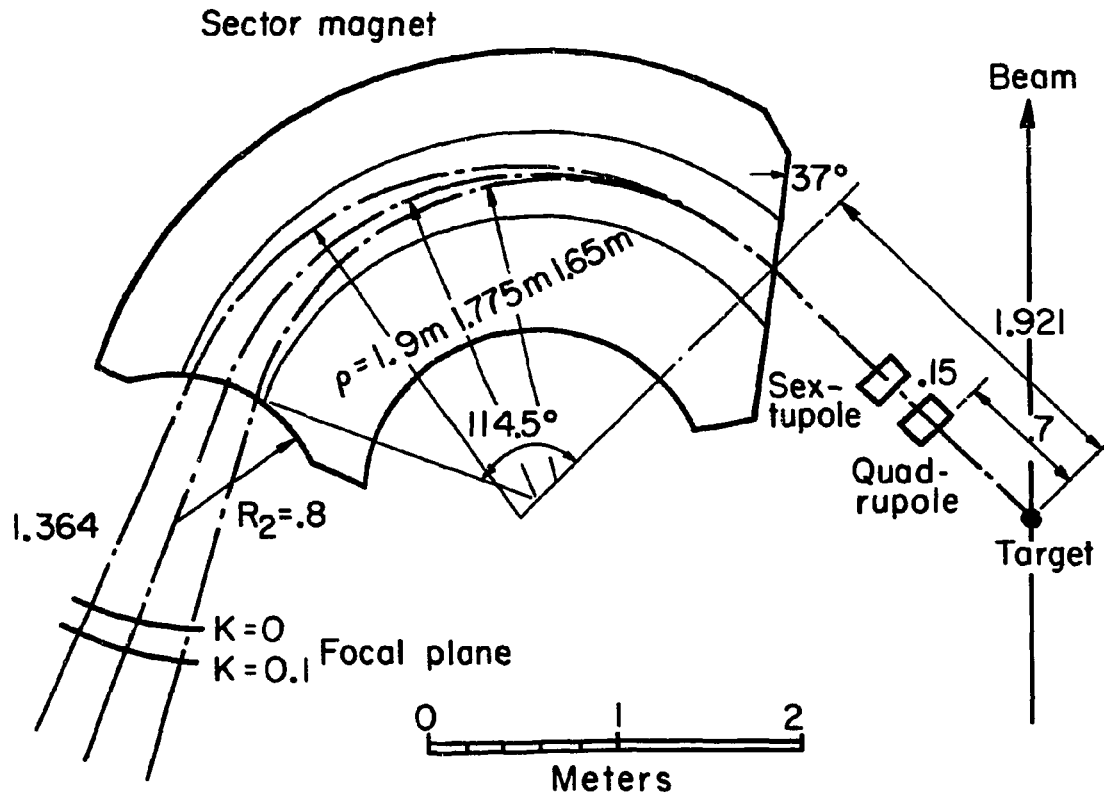
Fig. 19. The layout of the existing Lawrence Berkeley Laboratory
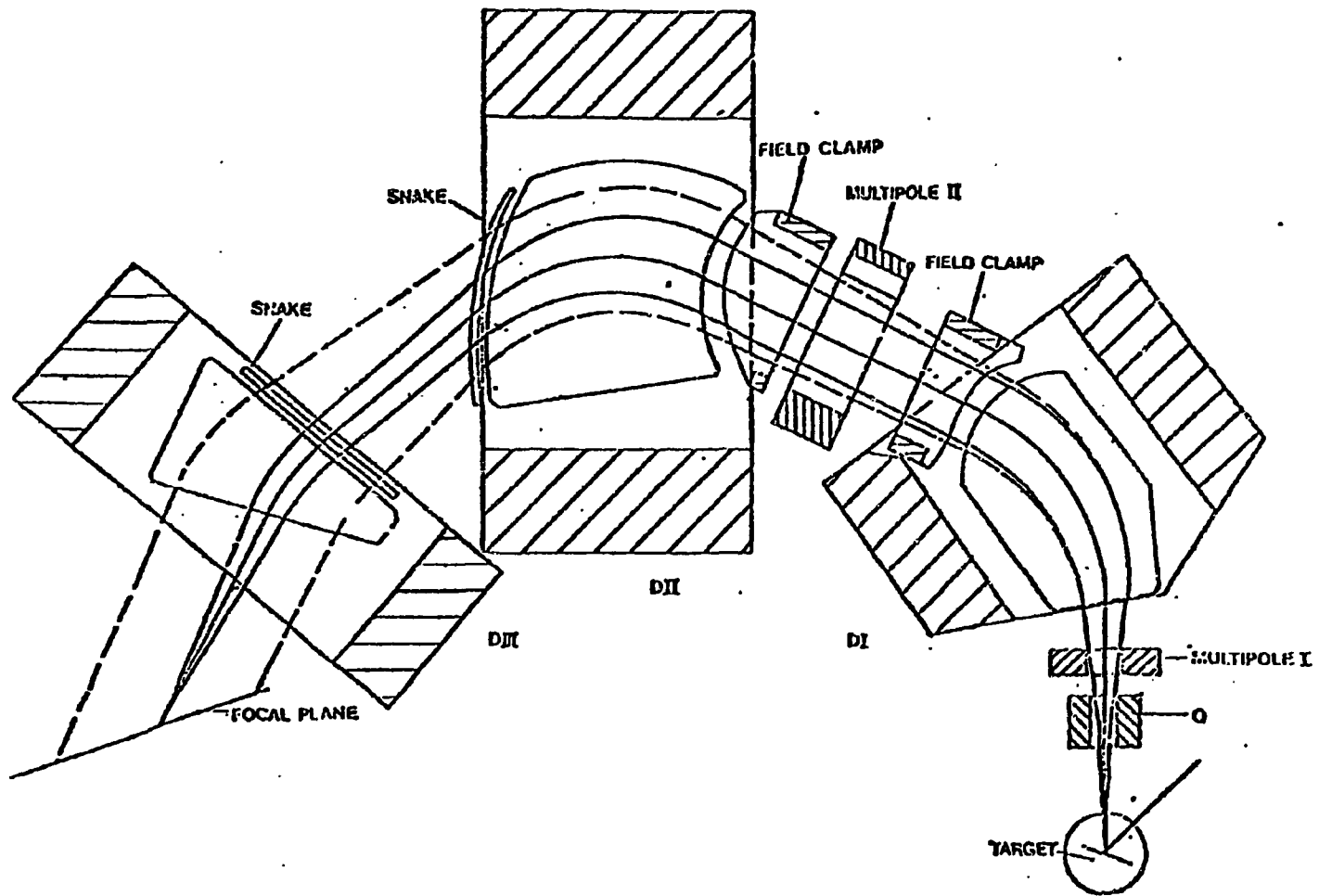spectrograph (Ref. 4).

Fig. 20.   The layout of the Groningen type Q3D spectrograph (Ref. 49).

54

be a proven device when ordered for the new tandem. However, like the QSD magnet this version of the Q3D has a vertical magnification larger than desirable.

c) Various new versions of the split-pole spectrograph have been suggested by H. A. Enge[48] which retain the basic simplicity and ease of operation of the split-pole spectrograph. Figure 21 shows the layout of the QSP design which provides an increased solid angle by adding a quadrupole before the dipole magnet and by a more complex shape of the field boundaries. The version QSP-N has particle orbits normal to the focal plane. It should be noted that it may be possible to upgrade either the existing ORNL split-pole or Elbek magnets to either a QSP or QSP-N device. However, such a converted magnet would likely still retain some of the limitations of the present spectrographs.

d) As indicated by the Jülich magnet, various other combinations of Q and D can be applied to good (although expensive) advantage. For example a QDMDQ spectrograph for the Indiana cyclotron (shown in Fig. 22) provides a solid angle of 4.8 msr, dispersion of 15, and vertical magnification of about 1.[50] Another example is a combination QD and Q3D spectrograph which could provide either low or high dispersion together with a large solid angle and straight focal plane.[44] Various combinations of magnetic elements which might satisfy the needs of a heavy ion spectrograph, therefore, could be further explored.

e) The usual concepts for designing conventional spectrographs can be abandoned in favor of superconducting devices which have the promise of providing extremely large solid angles. A spectrograph consisting of a superconducting quadrupole and dipole has been proposed for the Bevalac at Berkeley.[51] Large active focal plane detectors
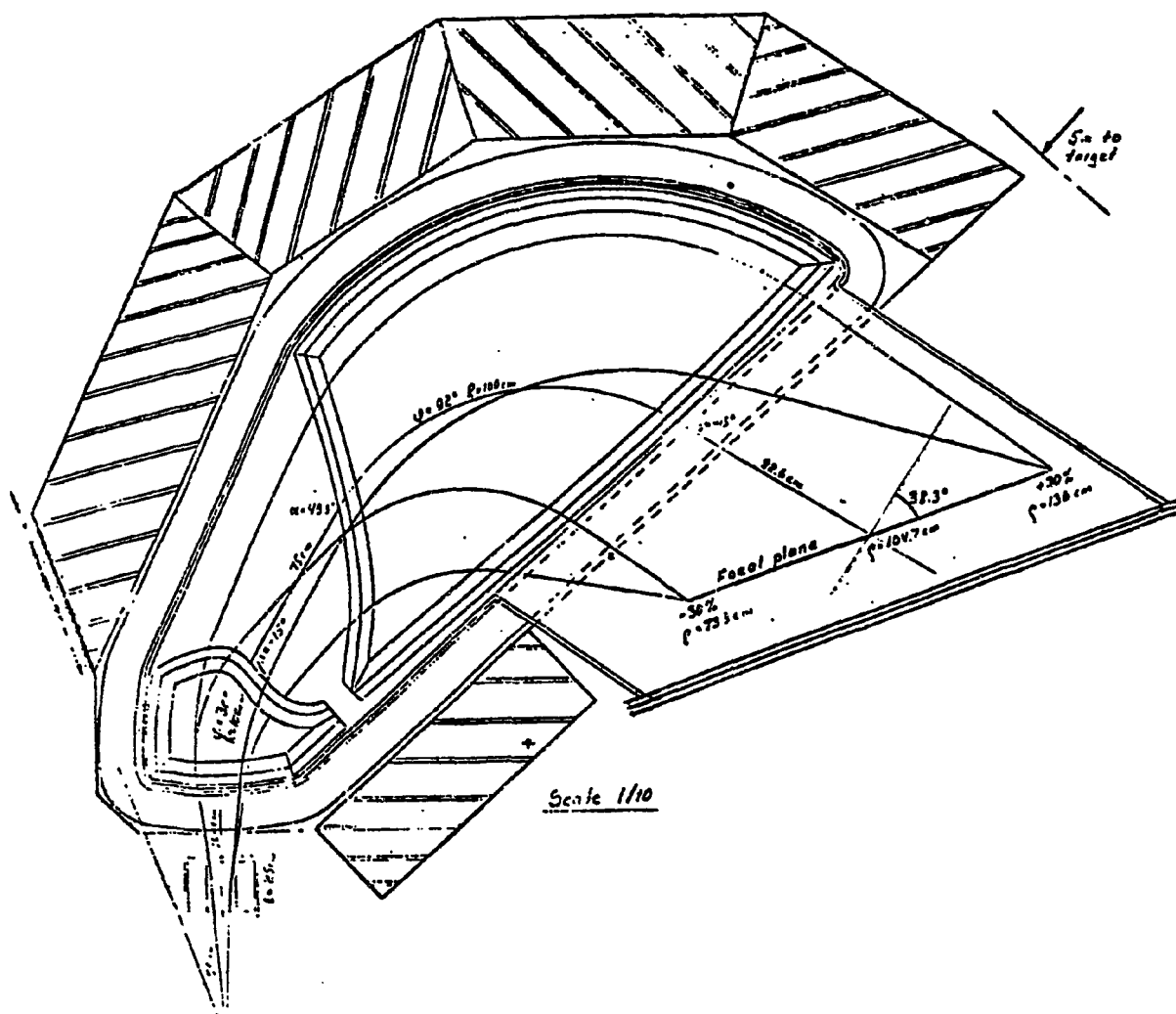
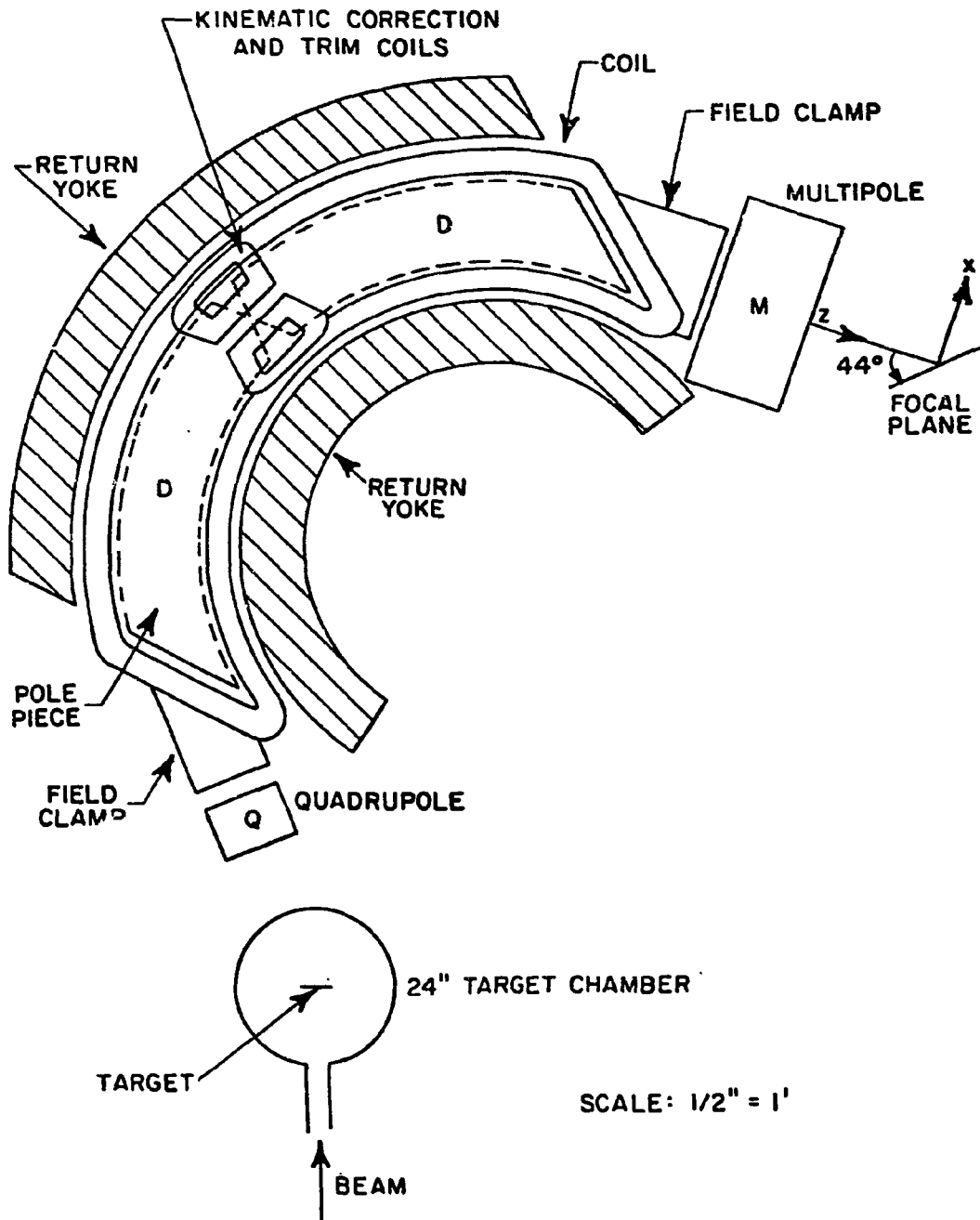Fig. 21. The layout of the proposed QSP spectrograph (Ref. 48).

Fig. 22. The layout of the University of Indiana QDDM spectrograph
(Ref. 50).

would then need to be used to measure the position and direction of the particle paths so that aberrations etc. could be corrected, and the angular distribution measured over the spectrograph opening. However, it is not clear whether or not such a device would be capable of providing the high resolution required for the 25 MV tandem.

Room temperature or superconducting solenoids are also devices that have been used in high energy physics to obtain very large solid angles. However, once again further study is needed to determine if such devices can achieve the high resolution desirable for a magnetic system located at the new accelerator.

If a major new spectrograph could be located where the present Elbek magnet is situated, some of the costs of a spectrograph installation would be saved. For example, the concrete floor has been made sufficiently strong to support the weight involved, and the magnet carriage could be used for the new spectrograph. The figure for the remaining costs will, of course, depend on the type of spectrograph chosen as the most appropriate, and on a detailed cost analysis. Modifying the Elbek spectrograph to a split-pole will probably cost at least $200,000. However, a really adequate magnet for the heavy ion facility probably requires construction of a new spectrograph. The cost of the basic instrument will be about $800,00 to $1.2 million, depending upon the design choice.

VIII. SUMMARY

The research potential of the new heavy ion facility requires a modern magnetic spectrograph in order to fully explore the rich variety

of phenomena expected from higher energy, heavy ion collisions.

Among the advantages for heavy ion detection provided by a spectrograph are the following:

    a)   The high energy resolution needed to match the excellent beam qualities of the new tandem (one of the unique characteristics of this machine).

    b)   Unmatched particle identification.

    c)   A large solid angle without loss of energy resolution.

    d)   Feasibility of zero-degree and very forward angle measurements.

A new spectrograph design must be closely coupled to the characteristics of the advanced focal plane detectors now available or expected in the near future. The possibility of upgrading the existing ORNL Elbek spectrograph should be explored. However, if a suitable modification of this magnet is not possible, then a new instrument should be obtained. The cost of an adequate new spectrograph will be approximately $1 million for the basic instrument. To this figure must be added the expense of the scattering chamber, detector system, and vacuum pumps.

REFERENCES

1. F. D. Becchetti, Proceedings of the International Conference on
    Nuclear Physics, Munich, Germany, August 27 - September 1, 1973
    (North Holland Publishing Company) 1973.

2. J. J. Kolata, private communication.

3. F. B. Selph, Lawrence Berkeley Laboratory, LBL-Engineering Note,
    CB 0401/M4196, September 1969, unpublished.

4. D. L. Hendrie, J. R. Meriwether, F. B. Selph, D. W. Morris,
    W. S. Flood, and B. G. Harvey, Lawrence Berkeley Laboratory,
    LBL Annual Report 1970, UCRL-20426, p. 280, unpublished.

5. M. J. Le Vine and H. A. Enge, BAPS 15, 1688 (1970).

6. C. H. Wiedner, M. Goldschmidt, D. Tieck, H. A. Enge, and
    S. B. Kowalski, Nucl. Instrum. Meth. 105, 205 (1972).

7. G. C. Morrison, Nuclear Structure Facility (Daresbury) - User's
    Committee Report of Working Party on the Magnetic Spectrograph
    (1975), and private communication.

8. J. R. Erskine, T. H. Braid, and J. C. Stoltzfus, Nucl. Instrum.
    Meth. 135, 67 (1976).

9. F. S. Goulding and B. G. Harvey, Annual Review of Nuclear Science
    (1975) p. 167.

10. B. G. Harvey, J. Mahoney, F. G. Pühlhofer, F. S. Goulding,
    D. A. Landis, J. C. Faivre, D. G. Kovar, M. S. Zisman,
    J. A. Meriwether, S. W. Cosper, and D. L. Hendrie, Nucl. Instrum.
    104, 21 (1972).

11. D. Shapira, R. M. DeVries, H. W. Fulbright, J. Toke, and
     M. R. Clover, Nucl. Instrum. Meth. 129, 123 (1975).

12. D. L. Hendrie, private communication.

13. B. L. Cohen, Rev. Sci. Instrum. 30, 415 (1959).

14. C. E. Bemis, Jr., F. K. McGowan, J. L. C. Ford, Jr., W. T. Milner,
     P. H. Stelson, and R. L. Robinson, Phys. Rev. C8, 1466 (1973).

15. J. E. Spencer and H. A. Enge, Nucl. Instrum. Meth. 49, 181 (1967).

16. D. L. Hillis, E. E. Gross, D. C. Hensley, L. D. Rickertsen,
     C. R. Bingham, A. Scott, and F. T. Baker, Phys. Rev. Letts. 36,
     304 (1976).

17. J. Borggreen, B. Elbek, and L. Perch Nielsen, Nucl. Instrum. Meth.
     24, 1 (1963).

18. J. B. Ball, IEEE Trans. Nucl. Sci. NS-13 (4), 340 (1966).

19. J. L. C. Ford, Jr., J. Gomez del Campo, R. L. Robinson, P. H. Stelson,
     and S. T. Thornton, Nucl. Phys. A226, 189 (1974).

20. L. R. Greenwood, R. E. Segel, K. Raghunathan, M. A. Lee,
     H. T. Fortune, and J. R. Erskine, Phys. Rev. 12C, 156 (1975).

21. K. A. Erb, D. L. Hanson, R. J. Ascuitto, B. Sorensen, J. S. Vagen,
     and J. J. Kolata, Phys. Rev. Lett. 33, 1102 (1974).

22. G. C. Ball, W. G. Davies, J. S. Forester, and H. R. Andrews,
     Phys. Letts. 60B, 265 (1976).

23. L. F. Fifield, R. W. Zurmuhle, D. P. Balamuth, and J. W. Noe,
     Phys. Rev. C8, 2203 (1973).

24. E. J. Williams, Phys. Rev. Sol. A135, 105 (1932).

25. J. R. Alonso and B. G. Harvey, Lawrence Berkeley Laboratory, LBL-1698, May 1973.

26. P. Sigmund and K. B. Winterbon, Nucl. Instrum. Meth. 119, 546 (1974).

27. R. O. Sayer, "SWIMS" A Small-Angle Multiple Scattering Computer Code, ORNL/CSD/TM-2, 1976.

28. J. D. Jackson, Classical Electrodynamics, Wiley Publishing Co. (1963) p. 458.

29. J. Rosenblatt, Rev. Sci. Instr. 31, 578 (1960).

30. B. Sjogren, Nucl. Instrum. and Meth. 7, 876 (1960).

31. B. L. Cohen, Rev. Sci. Instr. 33, 85 (1962).

32. J. D. Larson and C. M. Jones, to be published.

33. J. Barrette, P. Braun-Munzinger, and C. K. Gelbke, Nucl. Instrum. Meth. 126, 181 (1975).

34. F. Pühlhofer, unpublished.

35. C. M. Jones, J. A. Biggerstaff, J. K. Bair, J. B. Ball, J. D. Larson, J. A. Martin, J. W. McConnell, W. T. Milner, J. A. Murray, and N. F. Ziegler, Technical Specification for a 25 MV Tandem Electrostatic Accelerator, ORNL-TM-4942, Oak Ridge National Laboratory, August 1975.

36. D. L. Hendrie, Chapter III-C in Nuclear Spectroscopy and Reactions, Vol. A, J. Cerny, Editor, Academic Press, 1975.

37. F. Pühlhofer, Gesellschaft fur Schwerionenforschung, GSI Report 73-3, 1973, p. 99.

38. H. D. Betz, Rev. Mod. Phys. 44, 465 (1972).

39. H. A. Enge, Rev. Sci. Instr. 29, 885 (1958).

40. H. G, Bohlen, B. Gebauer, W. von Oertzen, Hahn-Meitner Institute Report HMI-B 171, May 1975.

41. T. Walcher, Max Planck Institut fur Kernphysik, Heidelberg, MPI H-1974-V25, (1974).

42. H. G. Bohlen, H. Lettan, H. Ossenbrink, and W. von Oertzen, Hahn-Meitner Institut Jahresbericht 1975.

43. R. G. Markham and R. G. H. Robertson, Nuc. Instrum. Meth. 129, 131 (1975).

44. H. A. Enge, private communication.

45. E. E. Gross, Nucl. Instrum. Meth. 121, 297 (1974).

46. R. M. De Vries, D. Shapira, and M. R. Clover, BAPS 21, 1007 (1976) and private communication.

47. S. Martin and C. Mayer-Boricke, Kernforschungslage Jülich Report, August, 1972.

48. H. A. Enge, Workshop on Heavy Ion Instrumentation, Oak Ridge National Laboratory, October 1975, unpublished.

49. A. G. Drentje, H. A. Enge, and S. B. Kowalski, Nucl. Instrum. Meth. 122, 485 (1974).

50. R. D. Bent, D. G. Madland, J. D. Cossairt, A. D. Bacher, W. P. Jones, D. W. Miller, R. E. Pollock, and S. Schwandt, Indiana University Cyclotron Facility Report No. 1-73, March, 1973.

51. HISS, A Proposal for a Heavy Ion Spectrometer System at the
    Bevalac, Lawrence Berkeley Laboratory, 1975, unpublished.

.